

Informed Asymmetric Actor-Critic: Leveraging Privileged Signals Beyond Full-State Access

Daniel Ebi¹, Gaspard Lambrechts², Damien Ernst³, Klemens Böhm¹

¹Karlsruhe Institute of Technology, Karlsruhe, Germany

{daniel.ebi, klemens.boehm}@kit.edu

²McGill University and Mila Québec, Montreal, Canada

gaspard.lambrechts@mcgill.ca

³University of Liège, Liège, Belgium

dernst@uliege.be

Abstract

Asymmetric actor-critic methods are widely used in partially observable reinforcement learning, but typically assume full state observability to condition the critic during training, which is often unrealistic in practice. We introduce the informed asymmetric actor-critic framework, allowing the critic to be conditioned on arbitrary state-dependent privileged signals without requiring access to the full state. We show that any such privileged signal yields unbiased policy gradient estimates, substantially expanding the set of admissible privileged information. This raises the problem of selecting the most adequate privileged information in order to improve learning. For this purpose, we propose two novel informativeness criteria: a dependence-based test that can be applied prior to training, and a criterion based on improvements in value prediction accuracy that can be applied post-hoc. Empirical results on partially observable benchmark tasks and synthetic environments demonstrate that carefully selected privileged signals can match or outperform full-state asymmetric baselines while relying on strictly less state information.

1 Introduction

Reinforcement learning (RL) has emerged as a powerful tool for optimizing control policies in various domains, including the control of heating, ventilation, and air conditioning systems [1], energy systems [2, 3], autonomous driving [4], and robotics [5]. However, many real-world applications involve partial observability, where agents must make decisions based on incomplete and noisy observations. This setting is formalized by partially observable Markov decision processes (POMDPs) [6], where optimal actions depend on the history of past observations and actions.

To address this, RL methods for fully observable settings have been adapted by learning history-dependent policies, typically using recurrent neural networks (RNNs) that encode observation-action sequences [7, 8, 9, 10, 11, 12]. Many approaches compress these sequences into compact latent representations by introducing auxiliary learning objectives [13, 14, 15, 16, 17, 18, 19, 20, 21]. While these methods can, in principle, learn optimal policies, they assume the same level of observability during training and execution, constraining policy learning to the limited information available at deployment. Yet, in practice, this assumption is unnecessarily restrictive and possibly suboptimal. Many training environments provide additional information that is unavailable or impractical to access during execution, such as diagnostic sensors, internal simulator variables, or forecasted data. Importantly, these additional signals do not necessarily correspond to full access to the true underlying state, but they offer valuable insights that can improve training.

Several approaches have explored the use of privileged information. For example, some methods train privileged expert policies conditioned on the true state and then imitate them [22]. However, these methods often lack theoretical guarantees and may lead to suboptimal policies in POMDPs [23]. To mitigate this, Warrington et al. [23] propose constraining the expert policy to yield an optimal policy under partial observability. Another line of work exploits privileged information in model-based RL by constructing world models that summarize histories or integrate additional state signals. Examples include the Informed Dreamer [24], the Wasserstein Believer [25], and the Scaffolder [26].

Asymmetric actor-critic methods offer a promising approach for leveraging privileged information by conditioning the actor on observable histories and the critic on privileged signals during training [27, 28, 29]. Performance gains therefore arise from improved value estimation rather than richer actor inputs, as the actor never observes privileged signals. Pinto et al. [30] introduce an early asymmetric actor-critic method with a state-conditioned critic that achieves strong empirical performance. However, this formulation is generally ill-defined in POMDPs unless additional assumptions hold, such as state-decodability, where the belief over latent states collapses to a Dirac distribution given the history [31]. Baisero and Amato [31] address this issue by introducing the history-state value function to ensure unbiased gradients. Theoretical work has further established convergence guarantees for policy gradient and actor-critic methods in both fully and partially observable settings, including symmetric recurrent natural actor-critic methods using RNNs [7, 32, 33] and asymmetric settings with fixed agent state and linear function approximators [34] or tabular belief-weighted formulations [35]. However, existing asymmetric actor-critic approaches often assume full-state access, leaving the case of partial privileged signals underexplored.

In this work, we generalize asymmetric actor-critic methods by introducing the informed asymmetric actor-critic framework, which allows the critic to be conditioned on arbitrary state-dependent privileged signals, instead of requiring full-state access. We show that any state-conditioned additional information can be leveraged to ensure unbiased gradients in asymmetric actor-critic methods. This generalization allows for a broader class of privileged training-time signals, significantly extending the scope of asymmetric learning. It also raises a natural question: which privileged signals should be selected?

Given that any state-conditioned signal could, in theory, yield unbiased gradients, there is no inherent reason to prefer one signal over another. Selecting and evaluating useful signals therefore becomes a central problem in the next stage of asymmetric learning. We provide a first systematic answer to this question by introducing two novel informativeness criteria that assess the utility of additional signals w.r.t. value estimation: (i) a residual-based dependency measure, and (ii) a value-prediction-based measure to evaluate the effectiveness of privileged signals. We empirically validate our framework on benchmark tasks and synthetic informed POMDPs. Our results show that leveraging informative privileged signals significantly improves policy learning, challenging the assumption that full-state access is essential for effective asymmetric RL. This work opens the door to future research on the selection, evaluation, and integration of privileged information, offering new opportunities for improving RL performance in partially observable settings.

2 Background

In this section, we formally introduce partially observable Markov decision processes (POMDPs) and the symmetric actor-critic paradigm, and then describe the informed POMDP framework that motivates our informed asymmetric actor-critic framework.

2.1 Partially Observable Markov Decision Processes

A POMDP [6] models sequential decision-making under uncertainty as tuple $(\mathcal{S}, \mathcal{A}, \mathcal{O}, T, O, R, P, \gamma)$, where \mathcal{S} , \mathcal{A} , and \mathcal{O} denote the state, action, and observation spaces. The transition probabilities $T(s_{t+1}|s_t, a_t)$ describe the process dynamics. The agent emits observations via $O(o_t|s_t)$ at time t and selects actions a_t based on the observable history h_t , defined as the sequence of past observations and actions, including the current observation. Specifically, the history can be written as $h_t = (o_0, a_0, \dots, o_t)$. We define the set of observable histories as $\mathcal{H} = \bigcup_{t=0}^{\infty} \mathcal{H}_t$, where $\mathcal{H}_t \subseteq \mathcal{O} \times (\mathcal{A} \times \mathcal{O})^t$ is the set of histories of size t . The expected immediate reward of the agent is given by $R(s_t, a_t)$. We assume rewards are uniformly bounded by a constant $r_{\max} > 0$. P specifies the initial state distribution. The objective is to maximize the expected return $J(\pi) = \mathbb{E}^{\pi} [\sum_{t=0}^{\infty} \gamma^t R(s_t, a_t)]$, where $\pi(a_t|h_t)$ denotes a history-dependent policy and $\gamma \in [0, 1]$ is a discount factor. The future return from time t is defined as $G_t = \sum_{k=0}^{\infty} \gamma^k R(s_{t+k}, a_{t+k})$, which leads to the history-based Q -function, the expected return given the current history and action,

$$Q^{\pi}(h_t, a_t) = \mathbb{E}_{s_{t+1:\infty}, a_{t+1:\infty}}^{\pi} [G_t \mid h_t, a_t],$$

and the corresponding history value function

$$V^{\pi}(h_t) = \sum_{a_t \in \mathcal{A}} \pi(a_t|h_t) Q^{\pi}(h_t, a_t).$$

2.2 Symmetric Actor-Critic Paradigm

Given a history-dependent policy π_θ parametrized by θ (actor), the policy gradient in a POMDP is given by [36, 37]

$$\nabla_\theta J(\pi_\theta) = \mathbb{E} \left[\sum_t \gamma^t Q^\pi(h_t, a_t) \nabla_\theta \log \pi_\theta(a_t | h_t) \right]. \quad (1)$$

In practice, this expectation is estimated via Monte Carlo by sampling histories and actions in the POMDP, which is known to yield high-variance estimates. It has been shown that subtracting any function of the history, referred to as a baseline, from the Q -function does not bias the gradient while potentially reducing variance. Commonly, the value function $V^\pi(h_t)$ is used as this baseline, yielding the advantage formulation

$$\nabla_\theta J(\pi_\theta) = \mathbb{E} \left[\sum_t \gamma^t A^\pi(h_t, a_t) \nabla_\theta \log \pi_\theta(a_t | h_t) \right], \quad (2)$$

where $A^\pi(h_t, a_t) = Q^\pi(h_t, a_t) - V^\pi(h_t)$ is called the advantage function. Unfortunately, the exact forms in Equations 1-2 involve the unknown functions $Q^\pi(\cdot)$ and $V^\pi(\cdot)$. The Q -function $Q^\pi(h_t, a_t)$ can in principle be estimated using a single Monte Carlo sample of G_t , but $V^\pi(h_t)$ cannot because the sampled G_t is not conditionally independent of a_t given h_t . Practitioners typically approximate $Q^\pi(\cdot)$ or $V^\pi(\cdot)$ with parametric functions Q_ϑ^π or V_ϑ^π (critic), using temporal difference (TD) learning. Since a baseline requires $V^\pi(\cdot)$, many algorithms avoid estimating Q^π directly and instead rely on an advantage estimator that uses only the critic, $\hat{A}_t = r_t + \gamma V_\vartheta^\pi(h_{t+1}) - V_\vartheta^\pi(h_t)$, where r_t is the observed reward at time t . This estimator of the advantage is unbiased if V_ϑ^π perfectly approximates V^π .

2.3 Informed POMDPs

Modeling the training-execution asymmetry, in which the critic observes additional state-dependent signals during training, but the policy at deployment relies only on observation-action histories, requires a framework that formalizes these signals without altering execution-time dynamics. The informed POMDP formalism [24] provides a principled approach by augmenting the standard POMDP with an information variable. Specifically, the informed POMDP introduces an information space \mathcal{I} and an information function $I : \mathcal{S} \rightarrow \Delta(\mathcal{I})$, which gives the probability to obtain information $i_t \in \mathcal{I}$ in the true state $s_t \in \mathcal{S}$. Hence, the informed POMDP is defined by the 10-tuple $(\mathcal{S}, \mathcal{A}, \mathcal{I}, \mathcal{O}, T, I, \tilde{O}, R, P, \gamma)$. In contrast to the standard POMDP, the observation function is defined as $\tilde{O} : \mathcal{I} \rightarrow \Delta(\mathcal{O})$ and denotes the probability to obtain $o_t \in \mathcal{O}$ given $i_t \in \mathcal{I}$. The defining assumption of the informed POMDP is that the observation o_t is conditionally independent of the true state s_t given the information i_t , i.e., $p(o_t | i_t, s_t) = \tilde{O}(o_t | i_t)$. The information variable can thus be interpreted as a latent mediator that captures all state-dependent information relevant for generating observations. Each informed POMDP induces an underlying execution POMDP defined as $(\mathcal{S}, \mathcal{A}, \mathcal{O}, T, O, R, P, \gamma)$, with observation function $O(o_t | s_t) = \int_{i_t \in \mathcal{I}} \tilde{O}(o_t | i_t) I(i_t | s_t) d i_t$, which governs the agent's interaction at deployment.

Remark 2.1. This formulation is not restrictive. Suppose an execution POMDP with observations $o_t \sim O(o_t | s_t)$. Then, for any auxiliary observation $o_t^+ \sim O^+(o_t^+ | s_t)$, it is always possible to define an information $i_t = (o_t, o_t^+)$ such that $p(i_t, o_t | s_t) = I(i_t | s_t) \tilde{O}(o_t | i_t)$ holds.

Thus, the conditional-independence assumption offers a convenient modeling abstraction for introducing an information variable that is at least as informative about the underlying state as the execution-time observation, while preserving full generality. As a result, the informed POMDP framework naturally subsumes both standard POMDPs and settings with additional training-time signals, making it particularly well-suited for modeling asymmetric learning scenarios.

3 Informed Asymmetric Actor-Critic

In this section, we develop an asymmetric actor-critic framework that leverages arbitrary state-conditioned information during training. Building on the informed POMDP paradigm, we introduce informed history-based Q - and value functions and derive an unbiased policy gradient estimator. Our formulation strictly generalizes the history-state critic of Baisero and Amato [31]: instead of requiring access to the full state, we show that any privileged signal $i_t \sim I(i_t | s_t)$ suffices to obtain unbiased value estimates, without imposing additional assumptions on the POMDP. This significantly broadens the class of training-time

signals that can be leveraged in asymmetric actor-critic methods, and motivates the question of how such signals should be selected.

3.1 Informed History-based Value Functions

Given an informed POMDP, we consider the following informed history-based reward

$$R(h_t, i_t, a_t) = \mathbb{E}_{s_t} [R(s_t, a_t) | h_t, i_t]. \quad (3)$$

This reward incorporates additional state-conditioned information available during training while remaining unbiased w.r.t. the standard history-based reward when taking expectations over $p(i_t | h_t)$.

Lemma 3.1 (Unbiasedness of the informed history-based reward). *In an informed POMDP, the informed history-based reward function $R(h_t, i_t, a_t)$ satisfies*

$$\mathbb{E}_{i_t} [R(h_t, i_t, a_t) | h_t] = R(h_t, a_t),$$

for all $h_t \in \mathcal{H}$ and $a_t \in \mathcal{A}$, where the expectation is taken under the belief $p(i_t | h_t)$.

Proof. Using the definition of the standard history-based reward function, i.e.,

$$R(h_t, a_t) = \mathbb{E}_{s_t} [R(s_t, a_t) | h_t] = \sum_{s_t \in \mathcal{S}} R(s_t, a_t) p(s_t | h_t),$$

and applying the law of total probability, we obtain:

$$\begin{aligned} R(h_t, a_t) &= \sum_{s_t \in \mathcal{S}} p(s_t | h_t) R(s_t, a_t) \\ &= \sum_{s_t \in \mathcal{S}} \left(\sum_{i_t \in \mathcal{I}} p(s_t | h_t, i_t) p(i_t | h_t) \right) R(s_t, a_t) \\ &= \sum_{i_t \in \mathcal{I}} \left(\sum_{s_t \in \mathcal{S}} R(s_t, a_t) p(s_t | h_t, i_t) \right) p(i_t | h_t) \\ &= \mathbb{E}_{i_t} \left[\mathbb{E}_{s_t} [R(s_t, a_t) | h_t, i_t] | h_t \right] \\ &= \mathbb{E}_{i_t} [R(h_t, i_t, a_t) | h_t]. \end{aligned}$$

This concludes the proof. \square

Informed history Q -function. We now introduce the informed history Q -function, which extends the history-state critic of Baisero and Amato [31] to arbitrary state-conditioned privileged signals:

$$Q^\pi(h_t, i_t, a_t) = \mathbb{E}_{s_{t+1:\infty}, a_{t+1:\infty}} [G_t | h_t, i_t, a_t].$$

This Q -function is an unbiased estimator of the standard history-based Q -function.

Lemma 3.2 (Unbiasedness of the informed history Q -function). *In an informed POMDP, the informed history Q -function satisfies*

$$\mathbb{E}_{i_t} [Q^\pi(h_t, i_t, a_t) | h_t] = Q^\pi(h_t, a_t),$$

for all $h_t \in \mathcal{H}$ and $a_t \in \mathcal{A}$.

Proof. Starting with the definition of the history Q -function and using the law of total expectation, we have:

$$\begin{aligned} Q^\pi(h_t, a_t) &= \mathbb{E}_{s_{t+1:\infty}, a_{t+1:\infty}} \left[\sum_{k=0}^{\infty} \gamma^k R(s_{t+k}, a_{t+k}) | h_t, a_t \right] \\ &= \mathbb{E}_{i_t} \left[\mathbb{E}_{s_{t+1:\infty}, a_{t+1:\infty}} \left[\sum_{k=0}^{\infty} \gamma^k R(s_{k+t}, a_{k+t}) | h_t, i_t, a_t \right] | h_t \right] \\ &= \mathbb{E}_{i_t} [Q^\pi(h_t, i_t, a_t) | h_t]. \end{aligned}$$

This concludes the proof. \square

Informed history value function. Based on the proposed informed history Q -function, we can define the informed history value function:

$$V^\pi(h_t, i_t) = \mathbb{E}_{s_{t+1:\infty}, a_{t+1:\infty}}^{\pi} [G_t | h_t, i_t], \quad (4)$$

which admits the time-invariant policy-based decomposition

$$V^\pi(h, i) = \sum_{a \in \mathcal{A}} \pi(a|h) Q^\pi(h, i, a). \quad (5)$$

The corresponding Bellman equation is

$$Q^\pi(h, i, a) = R(h, i, a) + \gamma \mathbb{E}_{o', i' | i, a} [V^\pi(h', i')], \quad (6)$$

where $h' = hao'$. Analogously to the Q -function case, the informed history value function is an unbiased estimator of the standard history value.

Lemma 3.3 (Unbiasedness of the informed history value function). *In an informed POMDP, the informed history value function satisfies for all $h_t \in \mathcal{H}$:*

$$\mathbb{E}_{i_t} [V^\pi(h_t, i_t) | h_t] = V^\pi(h_t).$$

Proof. Given the definition of the history value function, i.e.,

$$V^\pi(h_t) = \mathbb{E}_{s_{t+1:\infty}, a_{t+1:\infty}}^{\pi} \left[\sum_{k=0}^{\infty} \gamma^k R(s_{k+t}, a_{k+t}) | h_t \right],$$

and using the law of total expectation, we have:

$$\begin{aligned} V^\pi(h_t) &= \mathbb{E}_{s_{t+1:\infty}, a_{t+1:\infty}}^{\pi} \left[\sum_k \gamma^k R(s_{k+t}, a_{k+t}) | h_t \right] \\ &= \mathbb{E}_{i_t} \left[\mathbb{E}_{s_{t+1:\infty}, a_{t+1:\infty}}^{\pi} \left[\sum_k \gamma^k R(s_{k+t}, a_{k+t}) | h_t, i_t \right] | h_t \right] \\ &= \mathbb{E}_{i_t} [V^\pi(h_t, i_t) | h_t]. \end{aligned}$$

This concludes the proof. \square

As discussed by Baisero and Amato [31], the history h_t determines the agent's future behavior under a fixed policy, while the state governs the environment's rewards and dynamics. In our setting, the privileged signal i_t provides additional state-dependent context that can reduce the ambiguity about the underlying state given a fixed history. Formally, letting $H(s_t | h_t)$ denote the conditional entropy of the state, standard information-theoretic results imply $E_{i_t | h_t} [H(s_t | h_t, i_t)] \leq H(s_t | h_t)$, so conditioning on i_t never increases, and on average reduces, uncertainty about the true state. This does not guarantee that $V^\pi(h_t, i_t)$ is inherently easier to approximate than $V^\pi(h_t)$; rather, it is the conditional expectation of a return random variable whose variance may be lower. In particular, by the law of total variance applied to the return G_t , $E_{i_t | h_t} [\text{Var}(s_t | h_t, i_t)] \leq \text{Var}(s_t | h_t)$, so appropriate choice of i_t can reduce the variance of value targets.

When the privileged signal coincides with the full state, $i_t = s_t$, our formulation reduces to the history-state value function of Baisero and Amato [31] (cf. Corollary A.1 in Appendix A), showing that their framework is a special case of our more general formalization.

3.2 Informed Asymmetric Policy Gradient

Using the informed history-based Q -function, we define the informed asymmetric policy gradient

$$\nabla_{\theta}^{\text{IAAC}} J(\pi_{\theta}) = \mathbb{E} \left[\sum_{t=0}^{\infty} \gamma^t Q^\pi(h_t, i_t, a_t) \nabla_{\theta} \log \pi_{\theta}(a_t | h_t) \right],$$

where the policy π_{θ} depends only on the history h_t , while the critic may additionally condition on training-time information i_t .

Incorporating privileged state-conditioned information into the critic does not bias the policy gradient: for any choice of i_t , the informed asymmetric policy gradient coincides with the standard policy gradient.

Theorem 3.4 (Informed asymmetric policy gradient). *Given an informed POMDP, the informed asymmetric policy gradient is equivalent to the standard policy gradient:*

$$\nabla_{\theta}^{IAAC} J(\pi_{\theta}) = \nabla_{\theta} J(\pi_{\theta}).$$

Proof. Given Equation 1 and Lemma 3.2, we have

$$\begin{aligned} \nabla_{\theta} J(\pi_{\theta}) &= \mathbb{E} \left[\sum_t \gamma^t Q^{\pi}(h_t, a_t) \nabla_{\theta} \log \pi_{\theta}(a_t | h_t) \right] \\ &\stackrel{(a)}{=} \sum_t \gamma^t \mathbb{E}_{h_t, a_t} \left[Q^{\pi}(h_t, a_t) \nabla_{\theta} \log \pi_{\theta}(a_t | h_t) \right] \\ &\stackrel{(b)}{=} \sum_t \gamma^t \mathbb{E}_{h_t, a_t} \left[\mathbb{E}_{i_t} \left[Q^{\pi}(h_t, i_t, a_t) | h_t \right] \nabla_{\theta} \log \pi_{\theta}(a_t | h_t) \right] \\ &\stackrel{(c)}{=} \sum_t \gamma^t \mathbb{E}_{h_t, i_t, a_t} \left[Q^{\pi}(h_t, i_t, a_t) \nabla_{\theta} \log \pi_{\theta}(a_t | h_t) \right] \\ &\stackrel{(d)}{=} \mathbb{E} \left[\sum_t \gamma^t Q^{\pi}(h_t, i_t, a_t) \nabla_{\theta} \log \pi_{\theta}(a_t | h_t) \right] \\ &= \nabla_{\theta}^{IAAC} J(\pi_{\theta}). \end{aligned}$$

Here, (a) and (d) follow from linearity of expectation, (b) uses Lemma 3.2, and (c) applies the law of total expectation. This concludes the proof. \square

This result strictly generalizes prior work on asymmetric actor-critic methods. In particular, it recovers the asymmetric policy gradient of Baisero and Amato [31] as a special case when $i_t = s_t$ (cf. Corollary A.2). Hence, Theorem 3.4 extends asymmetric actor-critic theory beyond state-based critics and provides a formal justification for the use of arbitrary state-conditioned training-time signals.

Informed history critic. As in symmetric actor-critic methods, we learn a value function using TD learning, and we use the TD error to form a low-variance advantage estimate. The informed history critic $\hat{V} : \mathcal{H} \times \mathcal{I} \rightarrow \mathbb{R}$ additionally receives a privileged signal and approximates the informed history value $V^{\pi}(h_t, i_t)$. Combined with a history-dependent actor $\hat{\pi}_{\theta}(a_t | h_t)$, this yields the *informed asymmetric actor-critic (IAAC)*. The resulting policy gradient estimator is

$$\hat{\nabla}_{\theta}^{IAAC} J(\pi_{\theta}) = \mathbb{E} \left[\sum_t \gamma^t \hat{A}_t^{IAAC} \nabla_{\theta} \log \hat{\pi}_{\theta}(a_t | h_t) \right],$$

where \hat{A}_t^{IAAC} is computed using the informed history critic.

4 Informativeness of Privileged Signals

While the informed asymmetric actor-critic framework guarantees unbiased policy gradients for any state-conditioned privileged signals (cf. Theorem 3.4), not all such signals are equally useful for learning in practice. The choice of i_t can affect the critic's learning efficiency and stability, motivating the need for criteria to select the most informative signals.

Here, we focus on the informativeness of $i_t \in \mathcal{I}$ from the perspective of predicting future returns, which is the critic's primary role. To this end, we introduce two criteria that quantify the informativeness of privileged signals and enable systematic comparison across different choices of i_t .

4.1 Residual Informativeness

The utility of a privileged signal i_t in an informed critic depends on whether it provides information about future returns beyond what is already encoded in the observable history-action pair (h_t, a_t) . At the population level, this corresponds to the conditional independence (CI) hypothesis

$$\mathbb{H}_0^{\text{CI}} : G_t \perp\!\!\!\perp i_t | h_t, a_t,$$

which factorizes the joint distribution as

$$p(G_t, i_t, h_t, a_t) = p(h_t, a_t)p(G_t|h_t, a_t)p(i_t|h_t, a_t).$$

Rejecting \mathbb{H}_0^{CI} indicates that i_t provides additional, non-redundant information about future returns. One typically requires samples from both \mathbb{H}_0^{CI} and \mathbb{H}_1^{CI} to perform this test. Unfortunately, directly obtaining samples following \mathbb{H}_0^{CI} is generally infeasible. Instead, interaction with the environment yields samples from the unknown joint distribution $p(G_t, i_t, h_t, a_t) = p(h_t, a_t)p(G_t, i_t|h_t, a_t)$, where CI cannot be assumed. Sampling independently from $p(G_t|h_t, a_t)$ would require learning this conditional distribution, which is challenging for high-dimensional histories, and risks introducing noise into any direct test. To circumvent this, we first remove the predictable components of G_t and i_t explained by (h_t, a_t) and test for dependence in the residuals. As we explain below, testing residual independence provides insight into the independence of the original random variables, while simultaneously allowing sampling from a tractable approximation of $p(G_t|h_t, a_t)$.

Definition 4.1 (α -residual informativeness). Let G_t , i_t , h_t , and a_t be random variables with finite second moments. Define the conditional-mean residuals

$$e_{G_t} := G_t - \mathbb{E}[G_t|h_t, a_t], \quad e_{i_t} := i_t - \mathbb{E}[i_t|h_t, a_t].$$

A privileged signal i_t is α -residual-informative if a statistical test of independence rejects the null hypothesis

$$\mathbb{H}_0^{\text{res}} : e_{G_t} \perp\!\!\!\perp e_{i_t},$$

in favor of the alternative $\mathbb{H}_1^{\text{res}} : e_{G_t} \not\perp\!\!\!\perp e_{i_t}$, at significance level $\alpha > 0$.

CI implies residual independence, $\mathbb{H}_0^{\text{CI}} \Rightarrow \mathbb{H}_0^{\text{res}}$, but the converse need not hold in general [38]. Hence, the residual test provides a necessary, but not sufficient, condition for CI, which aligns with our goal of detecting whether i_t carries additional predictive information about G_t beyond (h_t, a_t) . This reduces the problem to testing whether the unexplained components of G_t and i_t remain statistically dependent. Testing $\mathbb{H}_0^{\text{res}}$ ideally requires samples from

$$p(e_{G_t}|h_t, a_t)p(e_{i_t}|h_t, a_t)p(h_t, a_t),$$

which, as with the original random variables, is generally intractable. To approximate a sample of G_t independent of i_t but with the correct conditional mean, we construct a surrogate \tilde{G}_t in two steps: (1) we draw from the marginal distribution $p(G_t)$ of G_t , which is readily available from the collected episodes; (2) we shift these samples to preserve the estimated conditional mean $\mathbb{E}[G_t|h_t, a_t]$. Thus,

$$\tilde{G}_t^{\text{null}} = \tilde{G}_t - \mathbb{E}[\tilde{G}_t] + \mathbb{E}[G_t|h_t, a_t].$$

By construction, the distribution of this sample exactly matches the first moment of the target distribution $p(G_t|h_t, a_t)$, while its higher-order moments follow those of the marginal distribution $p(G_t)$. The corresponding null residual

$$e_{\tilde{G}_t}^{\text{null}} := \tilde{G}_t^{\text{null}} - \mathbb{E}[G_t|h_t, a_t] = \tilde{G}_t - \mathbb{E}[\tilde{G}_t]$$

is therefore independent of e_{i_t} , satisfying $\mathbb{H}_0^{\text{res}}$.

Practical Implementation. In practice, we approximate the conditional expectations $\mathbb{E}[G_t|h_t, a_t]$ and $\mathbb{E}[i_t|h_t, a_t]$ using regression models capable of capturing nonlinear relationships (e.g., random forests or neural networks), since G_t and i_t typically exhibit nonlinear dependence. Histories are generally encoded using a recurrent network to produce a fixed-length representation $z_t = f_{\text{RNN}}(h_t)$, yielding residual estimates

$$\hat{e}_{G_t} := G_t - \hat{\mathbb{E}}[G_t|z_t, a_t], \quad \hat{e}_{i_t} := i_t - \hat{\mathbb{E}}[i_t|z_t, a_t], \quad (7)$$

and for the null sample, we have $\hat{e}_{\tilde{G}_t}^{\text{null}} := \tilde{G}_t - \hat{\mathbb{E}}[G_t|z_t, a_t]$. We quantify the dependence between \hat{e}_{G_t} and \hat{e}_{i_t} using a general dependency measure $\rho(\cdot, \cdot)$ (e.g., mutual information or Hilbert-Schmidt Independence Criterion). By design, $\rho(\hat{e}_{G_t}, \hat{e}_{i_t}) = 0$ under independence and increases with stronger dependence. To account for finite-sample variability and temporal correlations, we approximate the surrogate null by episode-wise permutation of the observed residuals. Residuals \hat{e}_{G_t} are shuffled across independently collected episodes while preserving the temporal order within each episode, which maintains the estimated conditional mean structure and respects intra-episode dependencies. Cross-fitting is used to prevent

overfitting: the dataset is split into K folds, with regressors trained on $K - 1$ folds and evaluated on the held-out fold.

We compute the empirical p -value with B permutations as

$$p = \frac{1 + \sum_{b=1}^B \mathbf{1}\{\rho(\hat{e}_{G_t}^{(b)}, \hat{e}_{i_t}^{(b)}) \geq \rho(\hat{e}_{G_t}, \hat{e}_{i_t})\}}{B + 1}, \quad (8)$$

where $\hat{e}_{G_t}^{(b)}, \hat{e}_{i_t}^{(b)}$ denote residuals under the b -th permutation and $\mathbf{1}\{\cdot\}$ is the indicator function, which equals 1 if the condition inside the braces holds and 0 otherwise. The privileged signal i_t is declared α -residual-informative if $p < \alpha$. Algorithm 1 summarizes the procedure.

Notably, the α -residual-informativeness criterion can be evaluated on episodes collected under any exploratory policy, without requiring a trained actor or critic. In particular, a random policy can be used, although coverage of the state-action space may be limited. This allows estimating the informativeness of privileged signals even before training and supports informed decisions about which signals to include. To obtain meaningful residuals, the history encoding function $f_{\text{RNN}}(\cdot)$ should be trained in advance to produce effective representations of past observations and actions.

Algorithm 1: α -Residual-Informativeness Test

Input: Independence measure $\rho(\cdot, \cdot)$, number of folds K , independently collected episodes $\{h_t, a_t, i_t, G_t\}_{t=0}^{T-1}$, number of permutations B , significance level α .
 Encode histories with recurrent network: $z_t = f_{\text{RNN}}(h_t)$.
 Partition data into K folds for cross-fitting
for each fold $k = 1$ to K **do**
 Train regression models on the $K - 1$ other folds.
 Predict $\hat{\mathbb{E}}[G_t | z_t, a_t]$ and $\hat{\mathbb{E}}[i_t | z_t, a_t]$ on the k -th fold.
 Compute residuals \hat{e}_{G_t} and \hat{e}_{i_t} on the k -th fold (Eq. 7).
end for
 Aggregate cross-fitted residuals across held-out folds.
 Compute observed dependence ρ_{obs} using $\rho(\cdot, \cdot)$.
for $b = 1$ to B **do**
 Permute residuals \hat{e}_{G_t} on episode-level.
 Compute $\rho_{\text{perm}}^{(b)}$ for permuted residuals.
end for
 Compute empirical p -value according to Eq. 8.
Output: Declare i_t α -residual-informative if $p < \alpha$.

4.2 Informativeness via Return Prediction Gain

Informativeness can also be assessed via the critic's predictive accuracy: a privileged signal is useful if its inclusion improves value estimation. Hence, this post-hoc criterion provides a quantitative measure of a signal's utility for return prediction. It only requires episodes collected under any fixed policy and does not depend on policy performance.

Consider a symmetric critic $\hat{Q}(h_t, a_t)$ and an informed asymmetric critic $\hat{Q}(h_t, i_t, a_t)$. For a set of N episodes $\{\tau_j\}_{j=1}^N$, we define the episode-level squared-error gain

$$L^{\tau_j} := \frac{1}{T_j} \sum_{t=0}^{T_j-1} \left((\hat{Q}(h_t, a_t) - G_t)^2 - (\hat{Q}(h_t, i_t, a_t) - G_t)^2 \right),$$

where T_j is the length of episode τ_j and G_t the true future return. $L^{\tau_j} > 0$ indicates that including i_t improves return prediction on that episode.

Definition 4.2 $((\epsilon, \delta)$ -prediction informativeness). A privileged signal i_t is said to be (ϵ, δ) -*prediction-informative* with $\epsilon \geq 0$ if a statistical test rejects the null hypothesis

$$\mathbb{H}_0 : \mathbb{E}[L^{\tau}] \leq \epsilon,$$

in favor of the alternative $\mathbb{H}_1 : \mathbb{E}[L^{\tau}] > \epsilon$, at significance level δ , based on the set of episode-level gains $\{L^{\tau_j}\}_{j=1}^N$.

Practical Implementation. In practice, the test procedure depends on the number of collected episodes N . For small sample sizes, we apply a one-sided bootstrap test: we resample $B > N$ episodes with replacement, compute bootstrap means $\{\bar{L}_b^*\}_{b=1}^B$, and estimate the empirical p -value as

$$p = \frac{1 + \sum_{b=1}^B \mathbf{1}\{\bar{L}_b^* \leq 0\}}{B + 1},$$

rejecting \mathbb{H}_0 if $p < \delta$. For larger sample sizes (e.g., $N > 1,000$), which we apply an one-sided t -test based on the sample mean \bar{L} and variance $\hat{\sigma}^2$. The test statistic is $t = \frac{\bar{L} - \epsilon}{\hat{\sigma}/\sqrt{N}}$, which under \mathbb{H}_0 follows a Student- t distribution with $N - 1$ degrees of freedom. We reject \mathbb{H}_0 if the corresponding one-sided p -value is below δ .

4.3 Selecting Privileged Signal Generators

Typically, one needs to select a signal generator from a candidate set $\mathcal{C} = \{I^{(m)}\}_{m=1}^M$, with each providing privileged information $i_t^{(m)} \sim I^{(m)}(\cdot|s_t)$. Different generators may encode distinct aspects of the state and are not directly comparable a priori.

Both proposed informativeness criteria support principled selection from \mathcal{C} via hypothesis testing. For each $I^{(m)}$, we evaluate the signal sequence $\{i_t^{(m)}\}_{0 \leq t < T}$ and deem the generator informative if the corresponding null hypothesis is rejected. In the pre-training setting, we apply the α -residual-informativeness test and select generators for which residual independence is rejected at significance level α . In the post-hoc setting, we apply the (ϵ, δ) -prediction-informativeness test and retain generators that yield a statistically significant improvement in value prediction accuracy ($\epsilon = 0$). Among informative candidates, one may select the generator with the largest effect size (or smallest p -value), yielding the signal that provides the strongest additional information about future returns under the respective criterion.

5 Experiments

We evaluate our informed asymmetric actor-critic framework along two complementary dimensions. First, we assess its learning performance on standard POMDP benchmarks against symmetric and asymmetric actor-critic baselines. Second, we validate the presented informativeness criteria in controlled informed POMDPs, where privileged signals can be systematically varied. We release our source code and experiments on GitHub¹ to ensure reproducibility.

5.1 Benchmark Performance

Environments. We use six benchmark navigation tasks from prior work [31] to evaluate the learning performance of our method: *Heaven-Hell-3*, *Shopping-5*, *Car-Flag*, *Cleaner*, *Memory-Four-Rooms-7x7*, and *Memory-Four-Rooms-9x9*. Each environment is formulated as a POMDP, and we define task-specific privileged signal accessible only to the critic. In *Heaven-Hell-3* and *Shopping-5*, the privileged signal corresponds to the Manhattan distance to the target. In *Car-Flag*, the critic additionally observes the agent’s velocity. For the other tasks, the privileged input consists of an expanded spatial observation of the agent’s surroundings. See Appendix C.1 for details.

Baselines. We compare our informed asymmetric actor-critic method, *informed-asymp-A2C*, against three advantage actor-critic (A2C) variants: (1) *A2C*, a symmetric approach using a history-based critic $\hat{V}(h)$; (2) *asymp-A2C-s*, an asymmetric variant with a state-based critic $\hat{V}(s)$; and (3) *asymp-A2C-hs*, an asymmetric variant with a history-state critic $\hat{V}(h, s)$. All policy networks receive identical inputs and never access privileged information. Model architectures and hyperparameters follow Baisero and Amato [31] to ensure a fair comparison and are detailed in Appendix D.1.

Results. Figure 1 reports the learning curves across all six benchmark tasks, showing episodic returns averaged over the last 100 episodes and aggregated across 20 independent runs. Across environments, *informed-asymp-A2C* consistently improves sample efficiency and training stability relative to *A2C*. In *Heaven-Hell-3*, *informed-asymp-A2C* exhibits strong performance relative to *A2C* and *asymp-A2C-s*, though it is slightly outperformed by *asymp-A2C-hs*. In *Shopping-5*, the informed asymmetric actor-critic converges

¹<https://github.com/EbiDa/informed-asymp-A2C>

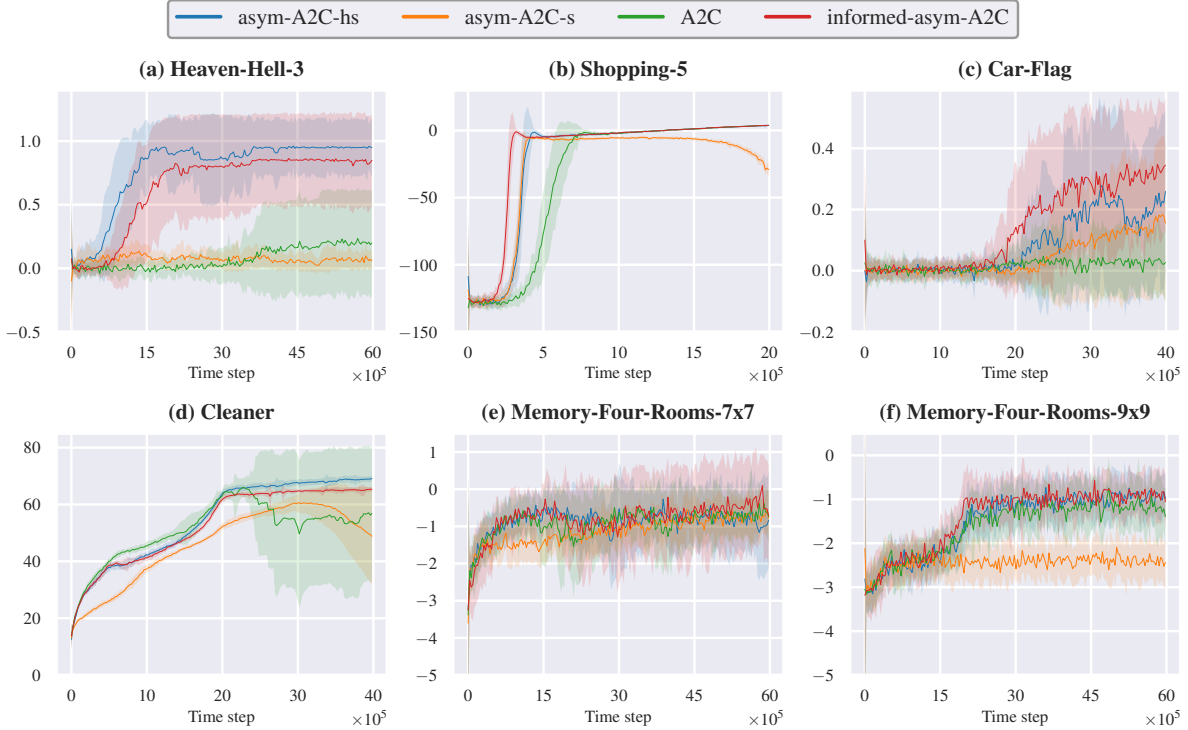


Figure 1: Learning performance on six benchmark navigation tasks. Curves show episodic returns averaged over the last 100 episodes, with means and standard deviations computed across 20 independent runs.

faster than *asym-A2C-hs* and achieves comparable asymptotic return. In *Car-Flag*, it outperforms all baselines in both convergence speed and asymptotic return. In *Cleaner*, *asym-A2C-hs* achieves marginally higher returns, but *informed-asym-A2C* converges at a similar rate with greater stability than *A2C*, which suffers a performance drop after 2.5 million steps. In the Memory-Four-Rooms tasks, *informed-asym-A2C* substantially outperforms both asymmetric baselines, particularly *asym-A2C-s*. Overall, *informed-asym-A2C* matches or surpasses the performance of *asym-A2C-hs* and/or achieves faster convergence in most tasks, demonstrating that appropriately structured privileged signals can match or outperform full-state informed critics while relying on strictly less additional information.

5.2 Validation of Informativeness Criteria

To empirically validate the proposed informativeness criteria in a controlled setting, we consider a distribution of synthetic informed POMDPs with finite state space ($|\mathcal{S}| = 20$), discrete action space ($|\mathcal{A}| = 4$), and continuous observation and privileged information spaces. Transition dynamics are generated following François-Lavet et al. [39] by sparsifying state-action transitions and normalizing to obtain valid probability distributions. Each state is associated with a latent Gaussian feature vector ($s_t \in \mathbb{R}^5$), and rewards are defined as linear functions of these features with weights w_r sampled uniformly from $[-1, 1]$. Privileged information is constructed by masking subsets of state features, while observations correspond to noisy subsets of this privileged signal. See Appendix C.2 for details on the environments.

Residual informativeness. For the residual-based criterion, we estimate dependence between return-prediction residuals and privileged-signal residuals via the Hilbert-Schmidt Independence Criterion (HSIC) [40] with Gaussian RBF kernels, where bandwidths are chosen via the median heuristic and a Nyström approximation [41] with 512 landmarks is applied for efficiency. We collect 250 episodes of length 25 under a random policy and perform episode-level permutation testing with $B = 1,000$ resamples. Conditional expectations are estimated via cross-fitting with a 100-tree random forest using 5-fold cross-validation. Observation-action histories are encoded with an RNN of hidden size 64, trained with temporal-difference learning on 100 training episodes.

Table 1: Comparison of privileged signal generators using residual-based and post-hoc prediction informativeness criteria across ten independent runs on a randomly sampled informed POMDP environment with reward weights $w_r = [0.0001, 0.0001, -0.0001, -1.0, 1.0]$. All values are reported as mean \pm standard deviation.

Privileged signal i_t	Residual Informativeness		Prediction Informativeness	
	$\rho_{\text{obs}} (\bar{x} \pm \hat{\sigma})$	$p\text{-value} (\bar{x} \pm \hat{\sigma})$	$L_\tau (\bar{x} \pm \hat{\sigma})$	$p\text{-value} (\bar{x} \pm \hat{\sigma})$
$i_t = [s_t^1, s_t^2]$	3.0e-05 \pm 8.1e-06	0.438 \pm 0.290	-1.4e-02 \pm 0.014	0.801 \pm 0.330
$i_t = [s_t^1, s_t^2, s_t^3]$	5.5e-05 \pm 1.9e-05	0.170 \pm 0.169	0.007 \pm 0.016	0.397 \pm 0.338
$i_t = [s_t^1, s_t^2, s_t^4]$	7.6e-05 \pm 3.2e-05	0.119 \pm 0.262	0.035 \pm 0.018	0.043 \pm 0.077
$i_t = [s_t^1, s_t^2, s_t^5]$	5.0e-05 \pm 1.5e-05	0.191 \pm 0.228	0.018 \pm 0.019	0.232 \pm 0.248
$i_t = [s_t^1, s_t^2, s_t^3, s_t^4]$	7.4e-05 \pm 2.4e-05	0.068 \pm 0.116	0.046 \pm 0.018	0.009 \pm 0.016
$i_t = [s_t^1, s_t^2, s_t^3, s_t^5]$	5.8e-05 \pm 1.5e-05	0.106 \pm 0.141	0.026 \pm 0.019	0.120 \pm 0.152
$i_t = [s_t^1, s_t^2, s_t^4, s_t^5]$	7.6e-05 \pm 2.1e-05	0.035 \pm 0.051	0.064 \pm 0.020	0.003 \pm 0.006
$i_t = [s_t^1, s_t^2, s_t^3, s_t^4, s_t^5]$	7.0e-05 \pm 1.8e-05	0.038 \pm 0.051	0.056 \pm 0.032	0.072 \pm 0.131

Post-hoc informativeness. For the post-hoc criterion, we train symmetric and informed critics with temporal-difference learning using 5-fold cross-validation on the same environments for 2,500 episodes of length 25. Histories are encoded with an RNN of hidden size 64, and the resulting fixed-length representation is concatenated with the privileged signal and fed into a linear output layer for value prediction. We evaluate episode-level gains in value prediction accuracy across held-out folds, with $\epsilon = 0$.

Results. Table 1 reports results for multiple privileged signal generators under both criteria across ten independent runs on a randomly sampled environment. In this setting, the agent observes noiseless $o_t = (s_t^1, s_t^2)$, while only a subset of state components (s_t^4, s_t^5) are relevant for the rewards, i.e., $w_r = [0.0001, 0.0001, -0.0001, -1.0, 1.0]$. Privileged signals that include these return-relevant components consistently exhibit stronger residual dependence and positive prediction gains. In contrast, signals containing only redundant or irrelevant (s_t^3) components yield weaker statistical evidence under both criteria. Interestingly, full-state access does not always achieve the best scores, highlighting that additional features can be uninformative when misaligned with return prediction. These results demonstrate that the two criteria provide complementary insights into signal informativeness, and that carefully selecting signals that capture return-relevant state components is most effective. Ablations and further results are provided in Appendix E.

6 Conclusion

We study asymmetric actor-critic learning under training-execution asymmetry and introduce the informed asymmetric actor-critic framework, which allows the critic to condition on state-dependent privileged signals unavailable at deployment while preserving unbiased policy gradients. This generalization moves asymmetric learning beyond full-state critics and shifts the focus from state access to identifying informative training-time signals. We propose two complementary criteria to assess informativeness before training and post hoc, and empirically demonstrate that appropriately chosen privileged signals can substantially improve learning and value estimation in POMDPs.

Future work may extend these criteria to account for signal complexity or direct policy effects, enabling better trade-offs between informativeness and model capacity for more robust and efficient learning under partial observability.

Acknowledgments

Daniel Ebi gratefully acknowledges the financial support of the *German Research Foundation* (DFG) as part of the *Research Training Group GRK 2153: Energy Status Data – Informatics Methods for its Collection, Analysis and Exploitation*. This work was carried out while Gaspard Lambrechts was a postdoctoral researcher at the University of Liège, supported by the *Fund for Scientific Research* (FNRS) from the *Wallonia-Brussels Federation* in Belgium. Additionally, this work was supported by the *Helmholtz Association Initiative and Networking Fund* on the HAICORE@KIT partition.

Impact Statement

This paper presents work whose goal is to advance the field of Machine Learning. There are many potential societal consequences of our work, none which we feel must be specifically highlighted here.

References

- [1] Khalil Al Sayed, Abhinandana Boodi, Rozbeh Sadeghian Broujeny, and Karim Beddiar. Reinforcement learning for HVAC control in intelligent buildings: A technical and conceptual review. *Journal of Building Engineering*, 95, 2024. ISSN 2352-7102.
- [2] Daniel Ebi, Edouard Fouché, Marco Heyden, and Klemens Böhm. MicroPPO: Safe power flow management in decentralized micro-grids with proximal policy optimization. In *2024 IEEE 11th International Conference on Data Science and Advanced Analytics (DSAA)*, pages 1–10, 2024.
- [3] Vincent François-Lavet, David Taralla, Damien Ernst, and Raphaël Fonteneau. Deep reinforcement learning solutions for energy microgrids management. In *European Workshop on Reinforcement Learning (EWRL 2016)*, 2016.
- [4] Ahmad Sallab, Mohammed Abdou, Etienne Perot, and Senthil Yogamani. Deep reinforcement learning framework for autonomous driving. *Electronic Imaging*, 2017:70–76, 01 2017.
- [5] Chen Tang, Ben Abbematteo, Jiaheng Hu, Rohan Chandra, Roberto Martín-Martín, and Peter Stone. Deep reinforcement learning for robotics: A survey of real-world successes. *Proceedings of the AAAI Conference on Artificial Intelligence*, 39(27):28694–28698, Apr. 2025.
- [6] Leslie Pack Kaelbling, Michael L Littman, and Anthony R Cassandra. Planning and acting in partially observable stochastic domains. *Artificial intelligence*, 101(1-2):99–134, 1998.
- [7] Semih Cayci and Atilla Eryilmaz. Recurrent natural policy gradient for POMDPs. In *ICML 2024 Workshop: Foundations of Reinforcement Learning and Control – Connections and Perspectives*, 2024.
- [8] Pengfei Zhu, Xin Li, Pascal Poupart, and Guanghui Miao. On improving deep reinforcement learning for PODMPs. *arXiv preprint arXiv:1704.07978*, 2017.
- [9] Marvin Zhang, Zoe McCarthy, Chelsea Finn, Sergey Levine, and Pieter Abbeel. Learning deep neural network policies with continuous memory states. In *2016 IEEE international conference on robotics and automation (ICRA)*, pages 520–527. IEEE, 2016.
- [10] Matthew Hausknecht and Peter Stone. Deep recurrent Q-learning for partially observable MDPs. In *2015 AAAI fall symposium series*, 2015.
- [11] Daan Wierstra, Alexander Förster, Jan Peters, and Jürgen Schmidhuber. Recurrent policy gradients. *Logic Journal of IGPL*, 18(5):620–634, 2010.
- [12] Bram Bakker. Reinforcement learning with long short-term memory. In T. Dietterich, S. Becker, and Z. Ghahramani, editors, *Advances in Neural Information Processing Systems*, volume 14. MIT Press, 2001.
- [13] Tianwei Ni, Benjamin Eysenbach, Erfan SeyedSalehi, Michel Ma, Clement Gehring, Aditya Mahajan, and Pierre-Luc Bacon. Bridging state and history representations: Understanding self-predictive RL. *arXiv preprint arXiv:2401.08898*, 2024.

[14] Jayakumar Subramanian, Amit Sinha, Raihan Seraj, and Aditya Mahajan. Approximate information state for approximate planning and reinforcement learning in partially observed systems. *Journal of Machine Learning Research*, 23(12):1–83, 2022.

[15] Alex X Lee, Anusha Nagabandi, Pieter Abbeel, and Sergey Levine. Stochastic latent actor-critic: Deep reinforcement learning with a latent variable model. *Advances in Neural Information Processing Systems*, 33:741–752, 2020.

[16] Zhaohan Daniel Guo, Bernardo Avila Pires, Bilal Piot, Jean-Bastien Grill, Florent Altché, Rémi Munos, and Mohammad Gheshlaghi Azar. Bootstrap latent-predictive representations for multitask reinforcement learning. In *International Conference on Machine Learning*, pages 3875–3886. PMLR, 2020.

[17] Dongqi Han, Kenji Doya, and Jun Tani. Variational recurrent models for solving partially observable control tasks. *arXiv preprint arXiv:1912.10703*, 2019.

[18] Karol Gregor, Danilo Jimenez Rezende, Frederic Besse, Yan Wu, Hamza Merzic, and Aaron van den Oord. Shaping belief states with generative environment models for RL. *Advances in Neural Information Processing Systems*, 32, 2019.

[19] Zhaohan Daniel Guo, Mohammad Gheshlaghi Azar, Bilal Piot, Bernardo A Pires, and Rémi Munos. Neural predictive belief representations. *arXiv preprint arXiv:1811.06407*, 2018.

[20] Lars Buesing, Theophane Weber, Sébastien Racaniere, SM Eslami, Danilo Rezende, David P Reichert, Fabio Viola, Frederic Besse, Karol Gregor, Demis Hassabis, et al. Learning and querying fast generative models for reinforcement learning. *arXiv preprint arXiv:1802.03006*, 2018.

[21] Maximilian Igl, Luisa Zintgraf, Tuan Anh Le, Frank Wood, and Shimon Whiteson. Deep variational reinforcement learning for POMDPs. In *International conference on machine learning*, pages 2117–2126. PMLR, 2018.

[22] Sanjiban Choudhury, Mohak Bhardwaj, Sankalp Arora, Ashish Kapoor, Gireeja Ranade, Sebastian Scherer, and Debadeepta Dey. Data-driven planning via imitation learning. *The International Journal of Robotics Research*, 37(13-14):1632–1672, 2018.

[23] Andrew Warrington, Jonathan W Lavington, Adam Scibior, Mark Schmidt, and Frank Wood. Robust asymmetric learning in POMDPs. In *International Conference on Machine Learning*, pages 11013–11023. PMLR, 2021.

[24] Gaspard Lambrechts, Adrien Bolland, and Damien Ernst. Informed POMDP: Leveraging additional information in model-based RL. *Reinforcement Learning Journal*, 2024.

[25] Raphaël Avalos, Florent Delgrange, Ann Nowe, Guillermo Perez, and Diederik M Roijers. The Wasserstein Believer: Learning belief updates for partially observable environments through reliable latent space models. In *The Twelfth International Conference on Learning Representations*, 2024.

[26] Edward S. Hu, James Springer, Oleh Rybkin, and Dinesh Jayaraman. Privileged sensing scaffolds reinforcement learning. In *The Twelfth International Conference on Learning Representations*, 2024.

[27] Miguel Vasco, Takuma Seno, Kenta Kawamoto, Kaushik Subramanian, Peter R Wurman, and Peter Stone. A super-human vision-based reinforcement learning agent for autonomous racing in Gran Turismo. *arXiv preprint arXiv:2406.12563*, 2024.

[28] Elia Kaufmann, Leonard Bauersfeld, Antonio Loquercio, Matthias Müller, Vladlen Koltun, and Davide Scaramuzza. Champion-level drone racing using deep reinforcement learning. *Nature*, 620(7976):982–987, 2023.

[29] Jonas Degrave, Federico Felici, Jonas Buchli, Michael Neunert, Brendan Tracey, Francesco Carpanese, Timo Ewalds, Roland Hafner, Abbas Abdolmaleki, Diego de Las Casas, et al. Magnetic control of tokamak plasmas through deep reinforcement learning. *Nature*, 602(7897):414–419, 2022.

[30] Lerrel Pinto, Marcin Andrychowicz, Peter Welinder, Wojciech Zaremba, and Pieter Abbeel. Asymmetric actor critic for image-based robot learning. *arXiv preprint arXiv:1710.06542*, 2017.

[31] Andrea Baisero and Christopher Amato. Unbiased asymmetric reinforcement learning under partial observability. In *Proceedings of the Conference on Autonomous Agents and Multiagent Systems*, 2022.

[32] Alekh Agarwal, Sham M. Kakade, Jason D. Lee, and Gaurav Mahajan. On the theory of policy gradient methods: optimality, approximation, and distribution shift. *J. Mach. Learn. Res.*, 22(1), 2021.

[33] Lingxiao Wang, Qi Cai, Zhuoran Yang, and Zhaoran Wang. Neural policy gradient methods: Global optimality and rates of convergence. In *8th International Conference on Learning Representations, ICLR 2020, Addis Ababa, Ethiopia, April 26-30*, 2020.

[34] Gaspard Lambrechts, Damien Ernst, and Aditya Mahajan. A theoretical justification for asymmetric actor-critic algorithms. In *Forty-second International Conference on Machine Learning*, 2025.

[35] Yang Cai, Xiangyu Liu, Argyris Oikonomou, and Kaiqing Zhang. Provable partially observable reinforcement learning with privileged information. *CoRR*, abs/2412.00985, 2024.

[36] Richard S. Sutton, David McAllester, Satinder Singh, and Yishay Mansour. Policy gradient methods for reinforcement learning with function approximation. In *Proceedings of the 13th International Conference on Neural Information Processing Systems, NIPS'99*, page 1057–1063, Cambridge, MA, USA, 1999. MIT Press.

[37] Daan Wierstra, Alexander Foerster, Jan Peters, and Jürgen Schmidhuber. Solving deep memory POMDPs with recurrent policy gradients. In Joaquim Marques de Sá, Luís A. Alexandre, Włodzisław Duch, and Danilo Mandic, editors, *Artificial Neural Networks – ICANN 2007*, pages 697–706, Berlin, Heidelberg, 2007. Springer Berlin Heidelberg.

[38] Hao Zhang, Yewei Xia, Kun Zhang, Shuigeng Zhou, and Jihong Guan. Conditional independence test based on residual similarity. *ACM Trans. Knowl. Discov. Data*, 17(8), 2023.

[39] Vincent François-Lavet, Guillaume Rabusseau, Joelle Pineau, Damien Ernst, and Raphael Fonteneau. On overfitting and asymptotic bias in batch reinforcement learning with partial observability. *J. Artif. Int. Res.*, 65(1):1–30, 2019.

[40] Arthur Gretton, Olivier Bousquet, Alex Smola, and Bernhard Schölkopf. Measuring statistical dependence with Hilbert-Schmidt Norms. In Sanjay Jain, Hans Ulrich Simon, and Etsuji Tomita, editors, *Algorithmic Learning Theory*, pages 63–77, Berlin, Heidelberg, 2005. Springer Berlin Heidelberg.

[41] Florian Kalinke and Zoltán Szabó. Nyström M-Hilbert-Schmidt independence criterion. In Robin J. Evans and Ilya Shpitser, editors, *Uncertainty in Artificial Intelligence, UAI 2023, July 31 - 4 August 2023, Pittsburgh, PA, USA*, volume 216 of *Proceedings of Machine Learning Research*, pages 1005–1015. PMLR, 2023.

[42] Hector Geffner and Blai Bonet. Solving large POMDPs using real time dynamic programming. In *Working Notes Fall AAAI Symposium on POMDPs*, 1998.

[43] Andrea Baisero. gym-pomdps: Gym environments from POMDP files. <https://github.com/abaisero/gym-pomdps>, 2019. Accessed: 2025-12-01.

[44] Hai Nguyen. POMDP Robot Domains. <https://github.com/hai-h-nguyen/pomdp-domains>, 2021. Accessed: 2025-12-01.

[45] Shuo Jiang and Christopher Amato. Multi-agent reinforcement learning with directed exploration and selective memory reuse. In *Proceedings of the ACM Symposium on Applied Computing*, pages 777–784, 03 2021.

[46] Andrea Baisero and Sammie Katt. gym-gridverse: Gridworld domains for fully and partially observable settings. <https://github.com/abaisero/gym-gridverse>, 2021. Accessed: 2025-12-01.

[47] Andrea Baisero and Sammie Katt. asym-porl: Asymmetric methods for partially observable reinforcement learning. <https://github.com/abaisero/asym-rlpo>, 2021. Accessed: 2025-12-01.

A Auxiliary Results

This section collects our auxiliary results.

Corollary A.1 (Relation of $V^\pi(h, i)$ to the history-state value function of Baisero and Amato [31]). *The informed history value function $V^\pi(h, i)$ reduces to the history-state value function for $i = s$, where $s \in \mathcal{S}$ denotes the true environment state. In particular,*

$$V^\pi(h, s) = \sum_{a \in \mathcal{A}} \pi(a|h) Q^\pi(h, s, a),$$

where the history-state action-value function is defined as

$$Q^\pi(h, s, a) = R(s, a) + \gamma E_{s', o'} [V^\pi(h', s')|s, a],$$

with $s' \sim T(s'|s, a)$, $o' \sim \tilde{O}(o'|s')$, $i' = s'$, and h' denoting the updated history resulting from appending action a and observation o' to h .

By Lemma 3.3, this formulation provides an alternative unbiased estimator of the history value function:

$$V^\pi(h) = E_s [V^\pi(h, s)|h],$$

as previously established by Baisero and Amato [31].

Corollary A.2 (Relation of $\nabla_\theta^{\text{AAC}} J(\pi_\theta)$ to the asymmetric policy gradient of Baisero and Amato [31]). *The informed asymmetric policy gradient $\nabla_\theta^{\text{AAC}} J(\pi_\theta)$ reduces to the asymmetric policy gradient introduced by Baisero and Amato [31] for $i = s$, where $s \in \mathcal{S}$ denotes the true environment state. In particular,*

$$\nabla_\theta^{\text{AC}} J(\pi_\theta) = E \left[\sum_{t=0}^{\infty} \gamma^t Q^\pi(h_t, s_t, a_t) \nabla_\theta \log \pi_\theta(a_t|h_t) \right].$$

Following Lemma 3.1 and 3.3, this formulation recovers an alternative asymmetric policy gradient estimator that is equivalent to the standard policy gradient:

$$\nabla_\theta^{\text{AC}} J(\pi_\theta) = \nabla_\theta J(\pi_\theta),$$

as established by Baisero and Amato [31].

B Analysis of the α -Residual-Informativeness Test

In this section, we detail the construction of the proposed α -residual-informativeness test and analyze its power.

B.1 Test Construction

In this subsection, we formalize the null distribution implicitly approximated by the permutation procedure used in the residual-based informativeness test. Our goal is to clarify how the proposed test relates to the conditional independence (CI) hypothesis

$$\mathbb{H}_0^{\text{CI}} : \quad G_t \perp\!\!\!\perp i_t | h_t, a_t.$$

Let G_t , i_t , h_t , and a_t be random variables with joint distribution $p(G_t, i_t, h_t, a_t)$ and finite second moments. Define the conditional-mean residuals

$$e_{G_t} := G_t - \mathbb{E}[G_t|h_t, a_t], \quad e_{i_t} := i_t - \mathbb{E}[i_t|h_t, a_t].$$

Proposition B.1. *If \mathbb{H}_0^{CI} holds, then*

$$e_{G_t} \perp\!\!\!\perp e_{i_t} | h_t, a_t.$$

Proof. Under \mathbb{H}_0^{CI} , the conditional joint distribution factorizes:

$$p(G_t, i_t | h_t, a_t) = p(G_t | h_t, a_t) p(i_t | h_t, a_t).$$

Subtracting measurable functions of (h_t, a_t) from each variable does not affect CI given (h_t, a_t) , so

$$p(e_{G_t}, e_{i_t} | h_t, a_t) = p(e_{G_t} | h_t, a_t) p(e_{i_t} | h_t, a_t).$$

This concludes the proof. \square

The converse does not hold in general [38]; thus, testing residual independence is a relaxation of CI testing.

Ideal residual null distribution. An exact test of $\mathbb{H}_0^{\text{res}} : e_{G_t} \perp\!\!\!\perp e_{i_t} \mid h_t, a_t$ would require samples from

$$p(h_t, a_t) p(e_{G_t} \mid h_t, a_t) p(e_{i_t} \mid h_t, a_t),$$

where the residual conditionals are induced by the joint law of (G_t, h_t, a_t) and (i_t, h_t, a_t) .

While (h_t, a_t, e_{i_t}) can be sampled from data once $\mathbb{E}[i_t \mid h_t, a_t]$ is estimated, obtaining independent samples from $p(e_{G_t} \mid h_t, a_t)$ is intractable because it requires sampling from the unknown return distribution conditioned on the full history h_t and action a_t .

First-moment-matching surrogate. To construct a tractable null distribution, we replace the original return G_t by a surrogate variable.

Assumption B.2 (Existence of a surrogate). There exists a random variable \tilde{G}_t defined on the same probability space such that

- (i) $\tilde{G}_t \stackrel{d}{=} G_t$ (same marginal distribution),
- (ii) $\tilde{G}_t \perp\!\!\!\perp i_t, h_t, a_t$ (independence from the privileged signal, history, and action),
- (iii) $\mathbb{E}[\tilde{G}_t^2] < \infty$ (finite second moment).

The surrogate null is then obtained by replacing G_t with

$$\tilde{G}_t^{\text{null}} := \tilde{G}_t - \mathbb{E}[\tilde{G}_t] + \mathbb{E}[G_t \mid h_t, a_t]. \quad (1)$$

The corresponding surrogate null residual is

$$e_{\tilde{G}_t}^{\text{null}} := \tilde{G}_t^{\text{null}} - \mathbb{E}[G_t \mid h_t, a_t] = \tilde{G}_t - \mathbb{E}[\tilde{G}_t].$$

Proposition B.3 (Properties of the surrogate residual). *For all (h_t, a_t) ,*

$$\mathbb{E}[e_{\tilde{G}_t}^{\text{null}} \mid h_t, a_t] = 0, \quad \text{and} \quad e_{\tilde{G}_t}^{\text{null}} \perp\!\!\!\perp i_t \mid h_t, a_t.$$

Proof. First, we prove zero conditional mean. By definition,

$$e_{\tilde{G}_t}^{\text{null}} = \tilde{G}_t - \mathbb{E}[\tilde{G}_t],$$

where $\mathbb{E}[\tilde{G}_t]$ is a constant. Taking the conditional expectation given (h_t, a_t) , yields

$$\mathbb{E}[e_{\tilde{G}_t}^{\text{null}} \mid h_t, a_t] = \mathbb{E}[\tilde{G}_t \mid h_t, a_t] - \mathbb{E}[\tilde{G}_t].$$

Since \tilde{G}_t is independent of (h_t, a_t) by Assumption B.2(ii),

$$\mathbb{E}[\tilde{G}_t \mid h_t, a_t] = \mathbb{E}[\tilde{G}_t].$$

Therefore,

$$\mathbb{E}[e_{\tilde{G}_t}^{\text{null}} \mid h_t, a_t] = 0.$$

Second, we show conditional independence from i_t . Again using

$$e_{\tilde{G}_t}^{\text{null}} = \tilde{G}_t - \mathbb{E}[\tilde{G}_t],$$

note that subtracting a constant does not affect independence relations. Thus, it suffices to show

$$\tilde{G}_t \perp\!\!\!\perp i_t \mid h_t, a_t.$$

For any measurable sets \mathcal{X}, \mathcal{Y} ,

$$p(\tilde{G}_t \in \mathcal{X}, i_t \in \mathcal{Y} \mid h_t, a_t) = \frac{p(\tilde{G}_t \in \mathcal{X}, i_t \in \mathcal{Y}, h_t, a_t)}{p(h_t, a_t)}. \quad (2)$$

Since \tilde{G}_t is independent of (h_t, a_t, i_t) ,

$$p(\tilde{G}_t \in \mathcal{X}, i_t \in \mathcal{Y}, h_t, a_t) = p(\tilde{G}_t \in \mathcal{X}) p(i_t \in \mathcal{Y}, h_t, a_t).$$

Substituting into Equation 2 gives

$$\begin{aligned} p(\tilde{G}_t \in \mathcal{X}, i_t \in \mathcal{Y} | h_t, a_t) &= p(\tilde{G}_t \in \mathcal{X}) \frac{p(i_t \in \mathcal{Y}, h_t, a_t)}{p(h_t, a_t)} \\ &= p(\tilde{G}_t \in \mathcal{X}) p(i_t \in \mathcal{Y} | h_t, a_t). \end{aligned}$$

Finally, because $\tilde{G}_t \perp\!\!\!\perp h_t, a_t$, we have

$$p(\tilde{G}_t \in \mathcal{X}) = p(\tilde{G}_t \in \mathcal{X} | h_t, a_t).$$

Therefore,

$$p(\tilde{G}_t \in \mathcal{X}, i_t \in \mathcal{Y} | h_t, a_t) = p(\tilde{G}_t \in \mathcal{X} | h_t, a_t) p(i_t \in \mathcal{Y} | h_t, a_t).$$

which establishes

$$\tilde{G}_t \perp\!\!\!\perp i_t | h_t, a_t.$$

Hence,

$$e_{\tilde{G}_t}^{\text{null}} \perp\!\!\!\perp i_t | h_t, a_t.$$

This concludes the proof. \square

Thus, the surrogate residual distribution

$$p(h_t, a_t) p(e_{\tilde{G}_t}^{\text{null}} | h_t, a_t) p(e_{i_t} | h_t, a_t)$$

matches the ideal residual-based null in the conditional mean of the residual while enforcing CI.

Therefore, the permutation test operates under a first-moment-matching surrogate null rather than the ideal CI null. Nevertheless, the test targets violations of residual independence and allows for identifying privileged signals that provide additional predictive information about returns. Moreover, the proposed test has the following interpretation:

- If CI holds, then residuals are conditionally independent given (h_t, a_t) , and the test does not reject $\mathbb{H}_0^{\text{res}}$ asymptotically under standard regularity conditions.
- If the test rejects $\mathbb{H}_0^{\text{res}}$, then i_t contains predictive information about the conditional mean of G_t beyond what is captured by $\mathbb{E}[G_t | h_t, a_t]$.
- The test does not guarantee full CI, only the absence of residual predictive information.

However, this notion of informativeness is in line with the objective of value-function learning, where conditional means, not full conditional distributions, determine optimal predictions.

B.2 Power Analysis of the α -Residual-Informativeness Test

This subsection studies how errors in the conditional expectation estimators affect the population dependence measure underlying the residual-informativeness test.

Regression error and residual perturbation. Let $m_G(h_t, a_t) = \mathbb{E}[G_t | h_t, a_t]$ and $m_i(h_t, a_t) = \mathbb{E}[i_t | h_t, a_t]$ denote the true conditional expectations, and let $\hat{m}_G(h_t, a_t), \hat{m}_i(h_t, a_t)$ be learned estimators. Define the regression errors

$$\Delta_{G_t} = m_G(h_t, a_t) - \hat{m}_G(h_t, a_t), \tag{3}$$

$$\Delta_{i_t} = m_i(h_t, a_t) - \hat{m}_i(h_t, a_t). \tag{4}$$

We assume the regression errors have finite second moments, i.e., $\mathbb{E}[\Delta_{G_t}^2] < \infty$, and $\mathbb{E}[\Delta_{i_t}^2] < \infty$.

The population residuals are

$$e_{G_t} = G_t - m_G(h_t, a_t), \quad e_{i_t} = i_t - m_i(h_t, a_t),$$

while the estimated residuals are

$$\hat{e}_{G_t} = G_t - \hat{m}_G(h_t, a_t) = e_{G_t} + \Delta_{G_t}, \quad \hat{e}_{i_t} = i_t - \hat{m}_i(h_t, a_t) = e_{i_t} + \Delta_{i_t}.$$

Throughout this section, we assume sample splitting, following the procedure described in Algorithm 1, so that regression estimation is independent of the dependence test.

Let $\rho(X, Y)$ denote a population dependence measure between square-integrable random variables. We impose the following stability condition.

Assumption B.4 (Lipschitz continuity in L^2). There exists a constant $L_\rho > 0$ such that for all X, X', Y, Y' with finite second moments,

$$|\rho(X, Y) - \rho(X', Y')| \leq L_\rho (\|X - X'\|_2 + \|Y - Y'\|_2),$$

where $\|Z\|_2 := \sqrt{\mathbb{E}[Z^2]}$.

This assumption is satisfied by many kernel- and distance-based dependence measures under additional regularity conditions (e.g., bounded Lipschitz kernels and finite second moments).

Applying Assumption B.4 with

$$(X, Y) = (e_{G_t}, e_{i_t}), \quad (X', Y') = (\hat{e}_{G_t}, \hat{e}_{i_t}),$$

yields

$$|\rho(e_{G_t}, e_{i_t}) - \rho(\hat{e}_{G_t}, \hat{e}_{i_t})| \leq L_\rho (\|\Delta_{G_t}\|_2 + \|\Delta_{i_t}\|_2). \quad (5)$$

Thus, regression error perturbs the population dependence measure by at most an additive margin proportional to the L^2 regression errors.

Implications for the detectable signal strength. Let q_α denote the rejection threshold of a level- α test based on an estimator of the dependence measure. Ignoring sampling variability for the moment and focusing on the underlying population quantities, the Lipschitz bound in Equation 5 implies

$$|\rho(e_{G_t}, e_{i_t}) - \rho(\hat{e}_{G_t}, \hat{e}_{i_t})| \leq \Delta_{\text{reg}}, \quad \Delta_{\text{reg}} = L_\rho (\|\Delta_{G_t}\|_2 + \|\Delta_{i_t}\|_2).$$

This yields two implications:

1. If the estimated dependence exceeds the rejection threshold, then the true residual dependence cannot be much smaller:

$$\rho(\hat{e}_{G_t}, \hat{e}_{i_t}) > q_\alpha \Rightarrow \rho(e_{G_t}, e_{i_t}) > q_\alpha - \Delta_{\text{reg}}.$$

Thus, false rejections due purely to regression error are controlled up to an additive tolerance Δ_{reg} .

2. Conversely, if the true residual dependence is sufficiently strong, then it remains detectable despite regression error perturbation:

$$\rho(e_{G_t}, e_{i_t}) > q_\alpha + \Delta_{\text{reg}} \Rightarrow \rho(\hat{e}_{G_t}, \hat{e}_{i_t}) > q_\alpha.$$

In other words, regression error effectively increases the minimum population dependence required for reliable detection by an additive margin Δ_{reg} . Alternatives with true residual dependence exceeding $q_\alpha + \Delta_{\text{reg}}$ remain well separated from the null, while alternatives within a Δ_{reg} -neighborhood of the threshold may become indistinguishable due to estimation error.

Note that the preceding argument describes population-level perturbation. In finite samples, additional variability in the test statistic introduces further uncertainty.

HSIC with Gaussian RBF kernels as dependency measure. We now consider ρ given by the population Hilbert-Schmidt Independence Criterion (HSIC) [40] with Gaussian RBF kernels

$$k(x, x') = \exp\left(-\frac{|x - x'|^2}{2\sigma_x^2}\right), \quad l(y, y') = \exp\left(-\frac{|y - y'|^2}{2\sigma_y^2}\right).$$

Gaussian RBF kernels are bounded and smooth, and are Lipschitz on bounded domains. Under finite second moments of the residuals (or sub-Gaussian tails), HSIC satisfies a bound of the form in Assumption B.4 under L^2 perturbations, with a constant that can be approximated by

$$L_\rho \approx C\left(\frac{1}{\sigma_x^2} + \frac{1}{\sigma_y^2}\right),$$

where C depends on the kernel bounds and residual moments.

In practice, σ_x and σ_y are often chosen by the median-pairwise-distance heuristic. This makes L_ρ data-dependent. Typically, residuals with larger typical pairwise distances lead to larger bandwidths and

hence smaller Lipschitz constants, which can reduce the sensitivity of HSIC to small regression-induced perturbations. This effect is heuristic rather than guaranteed, but commonly observed.

If the regression estimators are L^2 -consistent, i.e.,

$$\|\Delta_{G_t}\|_2 \rightarrow 0, \quad \|\Delta_{i_t}\|_2 \rightarrow 0,$$

as the regression sample size increases, then $\Delta_{\text{reg}} \rightarrow 0$. If these errors vanish at a rate sufficiently fast relative to the sampling variability of the HSIC estimator, then the residual-informativeness test based on estimated residuals inherits the asymptotic power of the oracle test. In this sense, regression error degrades power in a controlled and continuous manner and disappears in the large-sample limit under standard consistency conditions.

C Environments

This section details the partially observable environments used in our experiments.

C.1 Benchmark Environments

In this subsection, we present the partially observable benchmark environments used to assess the learning performance of the proposed informed asymmetric actor-critic method.

Heaven-Hell-3. The Heaven-Hell task [42, 43] is a partially observable navigation problem within a grid-world environment characterized by a corridor-like structure with a fork leading to three distinct terminal branches. Two of these branches correspond to terminal exits: one leading to a positive outcome (heaven) and the other to a negative outcome (hell). The third branch leads to a non-terminal location where the agent can interact with an oracle (referred to as a "priest") who provides information necessary to disambiguate the exits. The agent is initially unaware of which terminal corresponds to heaven. The underlying state includes both the agent's position and the true location of the heaven exit. As observation, however, the agent either perceives its own location or, when visiting the priest, receives an observation that reveals the location of heaven. We construct privileged partial information by adding to the agent's location its distance to the heaven terminal using Manhattan distance.

At each time step, the agent selects an action from the discrete set **NORTH, SOUTH, EAST, WEST**. The environment is deterministic, and movement is constrained by the grid-world layout. To solve the task optimally, the agent must first visit the priest to acquire the necessary information about the correct exit, then return to the fork and proceed to the identified heaven location.

The agent receives sparse feedback in the form of a terminal reward:

- a reward of 1.0 for exiting to heaven, and
- a reward of -1.0 for exiting to hell.

Shopping-5. The Shopping-5 environment [43] models another grid-world navigation task in which an agent must buy a forgotten item from a store. The environment is modeled as a two-dimensional grid-world of size 5×5 , with the item placed randomly at one of the grid cells. The agent begins at an arbitrary location and must locate and buy the item. While the agent's position is fully observable, the item's position is hidden and must be explicitly queried.

Hence, the full state encodes both the agent's position and the item's location, represented compactly as integers. Observations are similarly encoded, but are partial: at each time step, the agent observes either its own position or, upon executing a query, the position of the item. Similar to the Heaven-Hell task, we introduce a privileged partial by computing the current Manhattan distance between the agent and the item.

At each time step, the agent selects an action from the discrete set **{UP, DOWN, LEFT, RIGHT, QUERY, BUY}**. The four movement actions update the agent's position deterministically within the bounds of the grid. Executing the **QUERY** action returns the location of the item, but is subject to a cost. The **BUY** action attempts to purchase the item at the agent's current position; if executed in the correct cell, it completes the task successfully.

The environment provides a dense reward signal to encourage efficient behavior:

- a reward of -1.0 for moving,

- a reward of -2.0 for querying the item’s location,
- a reward of -5.0 for a **BUY** action in the wrong cell, and
- a reward of +10.0 for a **BUY** action in the correct cell.

Optimal behavior requires the agent to query the item’s location once, retain that information internally, and efficiently navigate to the target cell before executing a successful **BUY** action.

Car-Flag. The Car-Flag environment [44] models a continuous control task where an agent controls a car moving along a one-dimensional track via discrete force-control actions. At the two ends of the track are terminal flags: one representing a positive outcome (the good flag) and the other a negative outcome (the bad flag). Reaching either flag terminates the episode. Additionally, an intermediate information flag is placed along the track; when reached, it reveals the position of the good flag. While the task is conceptually similar to Heaven-Hell, key differences are the force-control and the position of the information flag.

Both the state and observation spaces are represented as three-dimensional real-valued vectors. The state includes the agent’s position, velocity, and the position of the good flag. The observation mirrors the state structure, but the third component (i.e., the good flag’s position) is masked, i.e., set to zero, when the agent is outside the observation range of the information flag; and the agent’s velocity is always hidden. In the informed setting, we provide the agent its velocity as a privileged partial signal.

At each time step, the agent selects an action from a discrete set of seven force-control inputs: **LEFT_HIGH**, **LEFT_MEDIUM**, **LEFT_LOW**, **RIGHT_LOW**, **RIGHT_MEDIUM**, **RIGHT_HIGH**, and **NONE**. These actions apply varying levels of acceleration to the left or right, or maintain zero acceleration.

The environment provides a sparse, terminal reward signal:

- a reward of 1.0 for reaching the good flag, and
- a reward of -1.0 for reaching the bad flag.

Optimal behavior requires the agent to first locate the information flag to identify the correct goal, then apply appropriate force controls to reach the good flag while avoiding the bad one.

Cleaner. Originally designed as a two-agent cooperative task, the Cleaner environment [45] is adapted in this work to a single-agent control problem via fully centralized training and execution. In this formulation, the joint actions and observations are constructed via the Cartesian product of the corresponding spaces of the two individual agents. The environment is a maze-like 13×13 grid-world in which two robots must collectively traverse and clean the entire area. The task is considered complete once every non-wall cell has been visited by at least one of the agents.

The full environment state is represented as a binary tensor of shape $13 \times 13 \times 5$, where each channel encodes the presence of: (i) a wall, (ii) a dirty cell, (iii) a cleaned cell, (iv) the first agent, and (v) the second agent. Each agent’s local observation is a $3 \times 3 \times 3$ binary tensor that captures the immediate neighborhood centered around the agent, including information about walls, dirty cells, and clean cells. As privileged input, the critic receives a $13 \times 13 \times 5$ tensor encoding the agent’s own position within the grid world, while masking out the position of the other agent by setting its corresponding cells to zero. Each agent independently selects from four movement actions: **UP**, **DOWN**, **LEFT**, and **RIGHT**. In the centralized setting, where both agents are controlled jointly, the action space is the Cartesian product of the individual action sets, yielding a total of 16 composite actions.

At each time step, the agent receives a reward proportional to the number of new cells cleaned during that step. The possible reward values are:

- a reward of 0.0 if no new cells are cleaned,
- a reward of 1.0 if one agent cleaned a new cell, and
- a reward of 2.0 if both agents cleaned a new cell.

Memory-Four-Rooms. The so-called Gridverse suite [46] defines a collection of partially observable environments in which agents interact within structured grid-worlds. In this work, we consider the 7×7 -Memory-Four-Room and 9×9 -Memory-Four-Room environments. While actions are encoded as categorical indices, both states and observations are structured representations comprising multiple semantically meaningful components. Importantly, these components differ between state and observation, and some are only available in the state representation. The key components are:

- Grid component: A tensor of shape $3 \times 7 \times 7$ for 7×7 -Memory-Four-Room or $3 \times 9 \times 9$ for 9×9 -Memory-Four-Room, where each channel encodes a semantic property of the environment (e.g., cell type, cell color, or status). The observation includes a rotated, agent-centric $3 \times 2 \times 3$ -view of this grid rendered from the first-person perspective of the agent. Cells obstructed by walls are occluded in the observation.
- Agent-ID-Grid component: A binary matrix of size 7×7 or 9×9 , respectively, indicating the agent’s absolute position. This component is included only in the state.
- Agent component: A three-dimensional categorical array encoding the agent’s position and orientation. In the state, this is expressed in absolute coordinates, while in the observation, it is provided relative to the agent’s perspective and is thus constant, and not necessary for control.

The environment contains a good exit, a bad exit, and a beacon, each placed randomly at the start of each episode. The beacon shares its color with the good exit, and successful task completion requires the agent to first locate the beacon, memorize its color, and then navigate to the exit of matching color while avoiding the bad exit.

As privileged input, the critic is provided with an agent-centered $3 \times 3 \times 5$ tensor, offering an expanded view of the agent’s local surroundings.

At each time step, the agent selects from the following discrete action set: `MOVE_FORWARD`, `MOVE_BACKWARD`, `MOVE_LEFT`, `MOVE_RIGHT`, `TURN_LEFT`, `TURN_RIGHT`, `PICK_N_DROP`, and `ACTUATE`. The `MOVE_` actions are interpreted relative to the agent’s orientation, while `TURN_` modifies the orientation itself. Although the action set includes `PICK_N_DROP` and `ACTUATE` for generality, these are no-ops in the Memory-Four-Rooms tasks, as there are no doors or pickable objects.

The reward signal is composed of the following terms:

- a living reward of -0.05 per time step,
- a reward of $+5.0$ for reaching the good exit, and
- a reward of -5.0 for reaching the bad exit.

C.2 Synthetic informed POMDPs

We generate a distribution of synthetic informed POMDP instances with a finite state space of size $|\mathcal{S}|$, a discrete action space of size $|\mathcal{A}|$, and continuous observation and information spaces. Following the methodology of François-Lavet et al. [39], transition probabilities are randomly assigned by setting each (s_t, a_t, s_{t+1}) -entry to zero with probability 0.75, and sampling uniformly from $[0, 1]$ otherwise. To ensure valid transitions, we assign a non-zero probability to a randomly chosen next state whenever all transitions from a given state-action pair are initially zero. We then normalize the probabilities so that they sum to one. Each state is associated with a Gaussian feature vector $s_t \in \mathbb{R}^{d_s}$ with $d_s \in \mathbb{Z}_{>0}$:

$$s_t \sim \mathcal{N}(\mathbf{0}, \sigma_s^2 \mathbf{I}_{d_s}),$$

where $\mathbf{0}$ is the d_s -dimensional zero vector and \mathbf{I}_{d_s} is the $d_s \times d_s$ identity matrix. Rewards are linear functions of the state features, with reward weights $w_r \in \mathbb{R}^{d_s}$ sampled uniformly from $[-1, 1]$ at initialization.

We first construct the privileged information $i_t \in \mathbb{R}^{d_i}$ by selecting a subset of $1 \leq d_i \leq d_s$ state features using a binary masking vector $m_i \in \{0, 1\}^{d_s}$ and applying a selection matrix $W_i \in \{0, 1\}^{d_i \times d_s}$:

$$i_t = W_i(m_i \odot s_t)$$

where \odot denotes element-wise multiplication. Observations $o_t \in \mathbb{R}^{d_o}$ are generated by masking a subset of $1 \leq d_o \leq d_i$ features from i_t using a binary masking vector $m_o \in \{0, 1\}^{d_i}$, applying a selection matrix $W_o \in \{0, 1\}^{d_o \times d_i}$ to the masked privileged signal, and adding Gaussian noise:

$$o_t = W_o(m_o \odot i_t) + \beta_o \epsilon_o, \quad \epsilon_o \sim \mathcal{N}(\mathbf{0}, \sigma_o^2 \mathbf{I}_{d_o}),$$

where $\beta_o \geq 0$ modulates the observation noise.

D Implementation Details

In this section, we detail parts of our implementation used in the evaluation. All experiments were conducted on a cluster node equipped with 64 cores running at 3.0 GHz and 72 GB of RAM allocated per task.

D.1 Model Architectures

In the following, we describe the model architectures employed for the actor and critic networks in each environment.

Benchmark tasks. For the benchmark tasks, we use the implementation [47] of environments and actor-critic methods provided by Baisero and Amato [31], extending them to the informed setting. In each task, a 128-dimensional single-layer gated recurrent unit (GRU) encodes the concatenated action and observation features into a history representation. While the actor and critic networks share this architectural component, their parameters are maintained separately. The subsequent actor and critic network components vary across environments as follows:

- For the Heaven-Hell-3 and Shopping-5 tasks, we employ a 64-dimensional embedding model to represent states, actions, and observations. Both the actor and critic networks consist of two-layer feedforward neural networks with 512 and 256 units, respectively, using ReLU activations in the hidden layers and a linear output layer.
- For the Car-Flag and Cleaner environments, actions are represented as one-hot encodings of their respective categorical indices. As the state and observation representations provided by these environments are already flattened and structurally simple, no additional embedding is applied. The actor’s and critic’s subsequent networks adopt the same architecture used for the Heaven-Hell-3 and Shopping-5 tasks.
- For the Memory-Four-Room tasks, the $3 \times 2 \times 3$ observation tensors are initially processed by an embedding layer that maps each categorical value to an 8-dimensional vector. The resulting embedded tensor is then flattened into a 144-dimensional feature vector, which serves as the observation input to both the actor and critic networks. Actions, provided as categorical indices, are represented using one-dimensional embedding layers. For the states, the grid component is first embedded and then concatenated with the agent-ID grid. A three-layer convolutional network subsequently processes this combined input. The output of the convolutional network is concatenated with the agent components. The actor and critic networks each consist of a hidden layer with 512 units using ReLU activation, followed by a linear output layer.

We encode the privileged information analogously to the observations. The embedded privileged information is then concatenated with the latent history representation before being passed to the task-specific feedforward neural network.

For each environment and method, we use the hyperparameter values recommended by Baisero and Amato [31] to ensure comparability with prior work. Table 2 summarizes the actor learning rate η_π , critic learning rate $\eta_{\hat{V}}$, and the initial negative-entropy weight λ_0 selected for each environment. Additionally, the following model hyperparameters are applied across all environments: discount factor is set to $\gamma = 0.99$, episodes are automatically terminated if they exceed 100 time steps; two episodes are sampled per gradient update; a frozen target network is used to stabilize critic training, with target parameters updated every 10,000 time steps; and the negative-entropy weight λ decays linearly over 2 million time steps to a final value equal to one-tenth of λ_0 .

Synthetic informed POMDPs. For the synthetic informed POMDP environments, the actor is implemented as a Gated recurrent unit (GRU) with hidden size $m_\pi = 64$, followed by a linear readout layer. Both the symmetric and informed history critics use a GRU of hidden size $m_{\hat{V}} = 64$ to produce fixed-length representations of the observation-action history, followed by a linear readout layer that outputs the value estimate. For the informed history critic, the GRU hidden state is concatenated with the privileged signal before being passed to the linear layer. The learning rate for both the actor and the critics is set to $\eta = 1 \times 10^{-4}$.

Across all environments, we use a fixed discount factor of $\gamma = 0.99$.

Table 2: Hyperparameters for the benchmark environments.

Environment	η_π	$\eta_{\hat{V}}$	λ_0
Heaven-Hell-3	0.001	0.001	0.1
Shopping-5	0.001	0.0003	3.0
Car-Flag	0.001	0.001	0.03
Cleaner	0.001	0.001	1.0
7 × 7-Memory-Four-Room	0.0003	0.001	0.1
9 × 9-Memory-Four-Room	0.001	0.0003	0.3

E Additional Experiments

This section summarizes our additional empirical results.

E.1 Effect of Privileged Signal Choice on Policy Performance

We study how different privileged signal generators affect the quality of the learned policy. To this end, we train a symmetric actor-critic baseline and multiple informed asymmetric actor-critic (IAAC) agents in the same fixed randomly sampled environment, each IAAC variant using a different privileged signal as described in Section 5.2. Each model is trained for 15,000 gradient steps, where every step uses a batch of 16 episodes. Every 50 gradient steps, we evaluate the current policy by estimating the mean episodic return over 50 evaluation episodes. All experiments are repeated with 10 random seeds. Figure 2 presents the actor loss, critic loss and episodic return on evaluation episodes during training for selected actor-critic variants, smoothed using a moving average over 500 episodes.

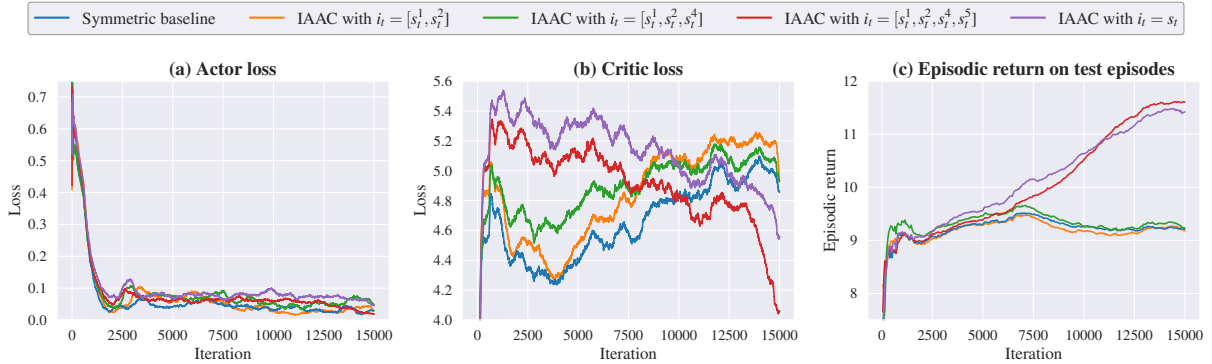


Figure 2: Learning performance of selected actor-critic variants on a randomly sampled informed POMDP. The curves depict (a) the actor loss, (b) the critic loss, and (c) episodic returns evaluated on 50 test episodes. The results are smoothed using a moving average over 500 gradient steps, with the means computed across 10 independent runs.

For each privileged signal generator, we compute the average gain in mean episodic return relative to the symmetric critic across all evaluation episodes during training, averaged over the 10 runs. In Figure 3, we plot this performance gain against the corresponding effect sizes of the two informativeness measures (observed HSIC and value prediction gain) to illustrate the relationship between signal informativeness and control performance. The informativeness tests are conducted offline using separate episodes collected with a random policy, allowing us to assess how well the proposed criteria serve as a proxy for downstream policy improvement.

The upper-right quadrant of the scatter plots highlights the most relevant privileged signal generators, combining high estimated informativeness with strong gains in mean episodic return. Signals such as $i_t = [s_t^1, s_t^2, s_t^4, s_t^5]$ and $i_t = s_t$ are consistently identified as informative (low p -values: 0.05-residual informativeness and (0, 0.05)- or (0, 0.1)-prediction informativeness) and yield the largest performance improvements. In contrast, some signals (e.g., $i_t = [s_t^1, s_t^2, s_t^3, s_t^4]$ or $i_t = [s_t^1, s_t^2, s_t^4]$) show strong effect sizes

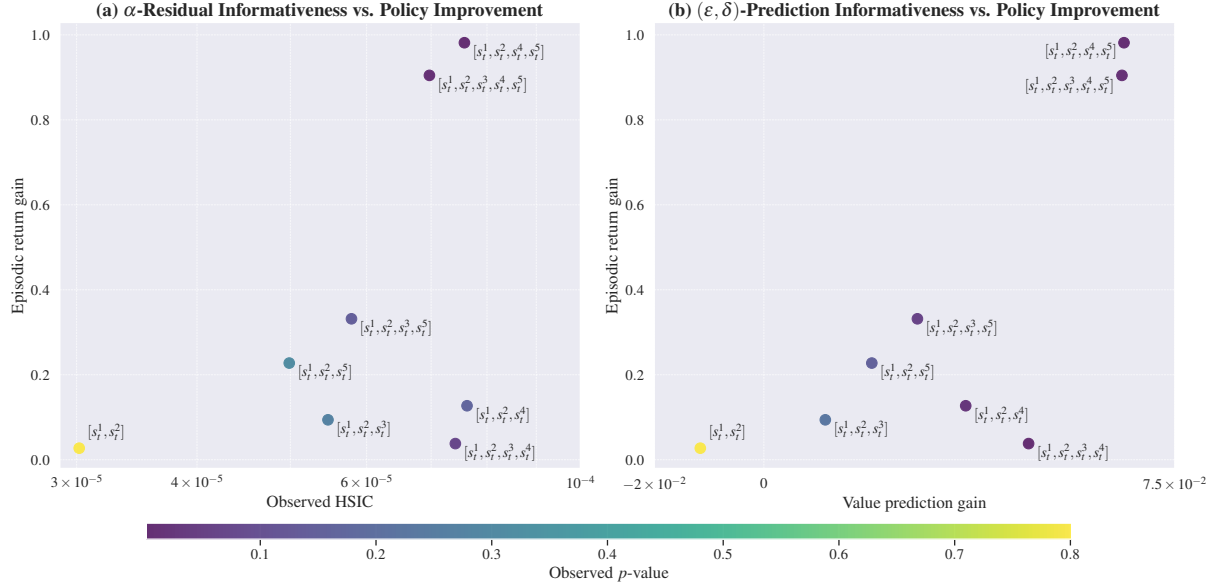


Figure 3: Relationship between estimated signal informativeness and downstream control performance. Each point corresponds to a distinct privileged signal configuration. The x-axis shows the effect size of the (a) residual-based informativeness measure (observed HSIC) and (b) post-hoc prediction informativeness measure (value prediction gain), while the y-axis shows the average gain in mean episodic return relative to a symmetric actor-critic baseline, aggregated over all evaluation episodes and averaged across 10 runs. Color of the point indicates the corresponding p -value of the respective informativeness test.

but smaller gains in episodic returns, while $i_t = [s_t^1, s_t^2, s_t^3, s_t^5]$ provides higher episodic gains despite lower measured informativeness. Signals identical to the observations ($i_t = o_t = [s_t^1, s_t^2]$) remain uninformative, in line with their limited contribution to policy improvement.

These results show that, while the proposed informativeness criteria are designed to quantify the predictive value of privileged signals for return estimation, they also serve as a reasonable proxy for downstream policy improvement. Notably, the tests are performed on episodes collected with a random policy, yet signals identified as informative tend to yield higher gains in episodic return during policy training. This suggests that value-based informativeness captures essential aspects of signals that facilitate control, while also highlighting the need for future research to develop criteria that directly assess a signal’s potential to enhance policy performance beyond value prediction. Interestingly, the full-state signal $i_t = s_t$ does not always produce the highest episodic return gains, further highlighting the practical relevance of the informed asymmetric actor-critic framework, which can exploit any state-dependent privileged information beyond full-state access.

E.2 Noisy observations

In addition to the noiseless observation setting studied in Section 5.2, we assess our informativeness criteria under noisy observation configurations. Recall that we generate observations by masking a subset of features from i_t and adding Gaussian noise modulated by $\beta_o \geq 0$.

Tables 3 and 4 report results for multiple privileged signal generators under noise levels $\beta_o = 0.1$ and $\beta_o = 0.5$, averaged over ten independent runs, using the α -residual-informativeness criterion and the post-hoc $(0, \delta)$ -prediction-informativeness measure, respectively. Increasing observation noise from $\beta_o = 0.0$ to $\beta_o = 0.1$ or $\beta_o = 0.5$ has only a minor impact on the relative ranking of privileged signals under both informativeness criteria. Signals that include the most return-relevant state components (notably those containing s_t^4) remain consistently identified as informative, with low p -values in both the residual-based and prediction tests. In contrast, signals lacking these components (e.g., $[s_t^1, s_t^2]$) continue to appear uninformative across noise levels. While effect sizes tend to increase slightly with higher noise for the truly informative signals the statistical conclusions remain generally unchanged.

This trend is intuitive. As observation noise increases, the history h_t becomes a less accurate proxy for the latent state, making the history-conditioned belief over states more uncertain. Privileged signals that

provide additional state-conditioned information can therefore explain a larger fraction of the remaining return variance, increasing their relative informativeness compared to the history alone.

An exception is $i_t = [s_t^1, s_t^2, s_t^3]$ under the residual-based criterion: its mean p -value increases noticeably with higher noise, making it less likely to be deemed as informative. In contrast, the post-hoc prediction criterion shows, on average, an increase in effect size for this signal at higher noise, indicating that it still provides useful predictive information even when the residual test becomes more conservative.

Table 3: Comparison of privileged signal generators using the residual-based informativeness criterion across ten independent runs on a randomly sampled informed POMDP environment with noisy observations. All values are reported as mean \pm standard deviation.

Privileged signal i_t	Noise factor $\beta_o = 0.1$		Noise factor $\beta_o = 0.5$	
	$\rho_{\text{obs}} (\bar{x} \pm \hat{\sigma})$	$p\text{-value} (\bar{x} \pm \hat{\sigma})$	$\rho_{\text{obs}} (\bar{x} \pm \hat{\sigma})$	$p\text{-value} (\bar{x} \pm \hat{\sigma})$
$i_t = [s_t^1, s_t^2]$	3.2e-05 \pm 1.2e-05	0.406 \pm 0.280	3.8e-05 \pm 1.8e-05	0.380 \pm 0.321
$i_t = [s_t^1, s_t^2, s_t^3]$	8.4e-05 \pm 3.5e-05	0.069 \pm 0.120	8.7e-05 \pm 3.9e-05	0.105 \pm 0.223
$i_t = [s_t^1, s_t^2, s_t^4]$	1.2e-04 \pm 3.7e-05	0.011 \pm 0.003	1.3e-04 \pm 3.8e-05	0.010 \pm 0.000
$i_t = [s_t^1, s_t^2, s_t^5]$	4.2e-05 \pm 1.5e-05	0.262 \pm 0.303	7.0e-05 \pm 4.0e-05	0.088 \pm 0.087
$i_t = [s_t^1, s_t^2, s_t^3, s_t^4]$	1.1e-04 \pm 3.7e-05	0.018 \pm 0.017	1.2e-04 \pm 3.7e-05	0.012 \pm 0.006
$i_t = [s_t^1, s_t^2, s_t^3, s_t^5]$	7.2e-05 \pm 2.7e-05	0.061 \pm 0.065	8.2e-05 \pm 3.5e-05	0.043 \pm 0.062
$i_t = [s_t^1, s_t^2, s_t^4, s_t^5]$	9.8e-05 \pm 2.8e-05	0.015 \pm 0.013	1.2e-04 \pm 4.0e-05	0.012 \pm 0.006
$i_t = [s_t^1, s_t^2, s_t^3, s_t^4, s_t^5]$	9.5e-05 \pm 3.0e-05	0.013 \pm 0.009	1.1e-04 \pm 3.5e-05	0.013 \pm 0.007

Table 4: Comparison of privileged signal generators using the post-hoc prediction informativeness criterion across ten independent runs on a randomly sampled informed POMDP environment with noisy observations. All values are reported as mean \pm standard deviation.

Privileged signal i_t	Noise factor $\beta_o = 0.1$		Noise factor $\beta_o = 0.5$	
	$L_\tau (\bar{x} \pm \hat{\sigma})$	$p\text{-value} (\bar{x} \pm \hat{\sigma})$	$L_\tau (\bar{x} \pm \hat{\sigma})$	$p\text{-value} (\bar{x} \pm \hat{\sigma})$
$i_t = [s_t^1, s_t^2]$	-0.013 \pm 0.014	0.788 \pm 0.343	0.004 \pm 0.012	0.456 \pm 0.298
$i_t = [s_t^1, s_t^2, s_t^3]$	0.007 \pm 0.016	0.384 \pm 0.330	0.021 \pm 0.014	0.081 \pm 0.084
$i_t = [s_t^1, s_t^2, s_t^4]$	0.035 \pm 0.018	0.041 \pm 0.071	0.049 \pm 0.017	0.001 \pm 0.002
$i_t = [s_t^1, s_t^2, s_t^5]$	0.019 \pm 0.019	0.219 \pm 0.231	0.036 \pm 0.017	0.030 \pm 0.031
$i_t = [s_t^1, s_t^2, s_t^3, s_t^4]$	0.046 \pm 0.018	0.009 \pm 0.016	0.057 \pm 0.017	3.2e-04 \pm 5.9e-04
$i_t = [s_t^1, s_t^2, s_t^3, s_t^5]$	0.027 \pm 0.019	0.110 \pm 0.137	0.043 \pm 0.017	0.010 \pm 0.011
$i_t = [s_t^1, s_t^2, s_t^4, s_t^5]$	0.064 \pm 0.020	0.003 \pm 0.006	0.077 \pm 0.018	1.5e-04 \pm 3.3e-04
$i_t = [s_t^1, s_t^2, s_t^3, s_t^4, s_t^5]$	0.056 \pm 0.032	0.073 \pm 0.131	0.068 \pm 0.030	0.022 \pm 0.041

E.3 Alternative feature subset

To assess the robustness of our results with respect to the choice of feature subsets used as observations, we repeat the informativeness tests from Section 5.2 using an alternative feature subset, with $\beta_o = 0.0$, while keeping the reward weights unchanged. This change in configuration also induces different signal generators, as we employ privileged signals of the form $i_t = (o_t, o_t^+)$. Comparing results across feature subsets allows us to evaluate the extent to which our findings depend on the particular choice of observable features.

Table 5 summarizes the performance of different privileged signal generators under both informativeness criteria, averaged over ten independent runs. For this analysis, the agent is provided with observations $o_t = [s_t^1, s_t^3]$.

In line with the previous experiments, signals that add little beyond the observation (e.g., $i_t = [s_t^1, s_t^3]$) are identified as uninformative by both criteria, with near-zero effect sizes and large p -values. Incorporating return-relevant components increases effect sizes. Under the post-hoc prediction criterion, signals containing

strongly reward-relevant features (i.e., s_t^4 and combinations including s_t^2 and s_t^4) yield clear and statistically significant gains, reflected in larger positive L_τ and small p -values. This supports earlier findings that signals which include the most reward-informative state dimensions are consistently ranked highest. The residual-based criterion remains more conservative, as in the original observation setting. Although the dependence measure ρ_{obs} generally increases when informative features are added, statistical significance at level $\alpha = 0.1$ is typically reached only for larger feature subsets (e.g., those containing both s_t^2 and s_t^4 , or the full state s_t).

Overall, the relative ordering of privileged signal generators is largely preserved across observation choices: signals containing the most reward-relevant state components remain the most informative under both criteria, although in some cases, higher significance levels are required to reach statistical significance.

Table 5: Comparison of privileged signal generators using residual-based and post-hoc prediction informativeness criteria across ten independent runs with observations $o_t = [s_t^1, s_t^3]$. All values are reported as mean \pm standard deviation.

Privileged signal i_t	Residual Informativeness		Prediction Informativeness	
	$\rho_{\text{obs}} (\bar{x} \pm \hat{\sigma})$	$p\text{-value} (\bar{x} \pm \hat{\sigma})$	$L_\tau (\bar{x} \pm \hat{\sigma})$	$p\text{-value} (\bar{x} \pm \hat{\sigma})$
$i_t = [s_t^1, s_t^3]$	2.4e-05 \pm 6.6e-06	0.673 \pm 0.273	-1.9e-02 \pm 0.010	0.973 \pm 0.041
$i_t = [s_t^1, s_t^2, s_t^3]$	4.9e-05 \pm 1.8e-05	0.240 \pm 0.315	0.023 \pm 0.010	0.052 \pm 0.099
$i_t = [s_t^1, s_t^3, s_t^4]$	4.5e-05 \pm 1.6e-05	0.314 \pm 0.329	0.008 \pm 0.015	0.307 \pm 0.345
$i_t = [s_t^1, s_t^3, s_t^5]$	5.8e-05 \pm 4.7e-05	0.307 \pm 0.275	0.004 \pm 0.014	0.390 \pm 0.342
$i_t = [s_t^1, s_t^2, s_t^3, s_t^4]$	6.2e-05 \pm 1.6e-05	0.057 \pm 0.082	0.057 \pm 0.012	0.003 \pm 0.008
$i_t = [s_t^1, s_t^2, s_t^3, s_t^5]$	5.4e-05 \pm 3.3e-05	0.240 \pm 0.279	0.039 \pm 0.012	0.016 \pm 0.031
$i_t = [s_t^1, s_t^3, s_t^4, s_t^5]$	6.8e-05 \pm 3.8e-05	0.080 \pm 0.076	0.031 \pm 0.018	0.107 \pm 0.192
$i_t = [s_t^1, s_t^2, s_t^3, s_t^4, s_t^5]$	6.3e-05 \pm 3.0e-05	0.071 \pm 0.102	0.068 \pm 0.019	0.006 \pm 0.013